Island Arc

Island Arc (2015) **24**, 317–341

Research Article

Paleoenvironments of the evolving Pliocene to early Pleistocene foreland basin in northwestern Taiwan: An example from the Dahan River section

TSUN-YOU PAN, ANDREW TIEN-SHUN LIN,* AND WEN-RONG CHI

Department of Earth Sciences, National Central University, No. 300, Zhongda Rd., Zhongli City, Taoyuan County 320, Taiwan (email: andrewl@ncu.edu.tw)

Abstract The overriding of the Luzon volcanic arc atop the underlying Chinese rifted-continental margin has caused the formation of the Taiwan mountain belts and a peripheral foreland basin west of the orogen since the late Miocene. In this study, lithofacies analysis and calcareous nannofossil biostratigraphic investigations of the Dahan River section in northwestern (NW) Taiwan were performed. Our results offer insights into the temporal evolution of the sedimentary environments and the competing effects of the sedimentation and basin tectonics of the NW Taiwan foreland basin from the Pliocene to early Pleistocene. Nannofossil biostratigraphic studies showed that the upper Kueichulin Formation and the overlying Chinshui Shale can be assigned to the NN15 biozone of the Pliocene age, and the Cholan Formation pertains to NN16–NN18 of the early Pleistocene. The NN15–NN16 boundary coincides roughly with the boundary of the Chinshui Shale and Cholan Formation. We recognized three major sedimentary environments in the studied foreland succession comprising the upper Kueichulin Formation, Chinshui Shale, Cholan Formation and Yangmei Formation, in ascending order. During the deposition of the upper Kueichulin Formation in the early Pliocene, the dominant environment was a wave- and tide-influenced open marine setting. During the late Pliocene, the environment deepened to an outer-offshore setting when the sediments of Chinshui Shale were accumulated. In the Pleistocene, the environment then shallowed to wave-dominated estuaries during the deposition of the lower Cholan Formation, and the basin was rapidly filled, generating a meandering and sandy braided river environment during the deposition of the upper Cholan to the Yangmei Formation. In summary, the evolution of sedimentary environments in the studied succession shows a deepening then a shallowing and coarsening upward trend during the period from the Pliocene to the Pleistocene, spanning the age from approximately 4 to 1 Ma.

Key words: foreland basin, Plio–Pleistocene, sedimentary environments, stratigraphy, Taiwan.

INTRODUCTION

A foreland basin is a wedge-shaped basin that is formed between an orogenic belt and the adjacent continental crust mainly in response to flexural subsidence resulting from orogenic and sediment loading (Dickinson 1974; DeCelles & Giles 1996; Naylor & Sinclair 2008). Studies of the paleoenvironments of foreland basins have not only yielded the paleogeography of foreland basins during the course of basin evolution, but have also shed light on the infilling processes of foreland basins (DeCelles & Giles 1996; Sinclair 1997). The Taiwan foreland basin, which is a classic example of peripheral foreland basins, has formed because of the tectonic loading of the Taiwan mountain belts (Covey 1984; Chen *et al*. 2001; Yu & Chou

*Correspondence.

Received 8 December 2014; accepted for publication 7 March 2015.

doi:10.1111/iar.12113

2001; Lin & Watts 2002) since the late Miocene because of arc–continent collision (Teng 1987, 1990). Covey (1986) proposed that the Taiwan foreland basin evolved from an underfilled to an overfilled sedimentary state, and this concept was cited in studies on foreland basins in the Alps, the Himalayas, and other regions (Fielding *et al.* 1993; Sinclair 1997; Najman *et al.* 2004).

Previous studies have reconstructed the filling processes of foreland deposits in central and southwestern (SW) Taiwan (Covey 1984; Tu & Chen 1984; Tu *et al.* 1984; Hong & Wang 1988; Wu & Wang 1989; Ting *et al.* 1991; Wu 1993; Yang & Hong 1994; Hong, 1997; Chen *et al.* 2001; Huang *et al.* 2002; Nagel *et al.* 2013). However, the foreland infilling processes that occurred from the Pliocene to the Pleistocene in northern Taiwan warrant detailed study. Along the Dahan River bed in northern Taiwan, a well-exposed foreland section that is approximately 2100 m in stratal thickness and contains continuous foreland basin strata is present. By conducting lithofacies analysis and biostratigraphic studies of the calcareous nannofossils obtained from this section, we interpreted the Pliocene to Pleistocene paleoenvironments of the foreland basin in northwestern (NW) Taiwan, and we present here a distinct overfilled sedimentary characteristic identified in foreland successions in central and SW Taiwan. Our paleoenvironment study conducted in the NW Taiwan foreland basin compliments previous studies that focused mainly on central and SW Taiwan, providing a holistic understanding of the sedimentary evolution of the entire Taiwan foreland basin. Our results also shed light on the interplay among eustatic sea-level changes, basin subsidence and sediment supply during the filling of a foreland basin.

GEOLOGICAL SETTING AND STRATIGRAPHY

The Dahan River section in northern Taiwan is located west of Tahsi Township in Taoyuan County (Fig. 1a). The studied stratigraphic section is located at the hanging wall of the Hsinchuang Fault. The stratigraphic base of the section (i.e. the late Miocene Kueichulin Formation) is cut at the north by the Taipei Fault, whereas the top of the section (i.e. the Pleistocene Yangmei Formation) is truncated at the south by the Hsintien Fault (Fig. 1b). The strata of the Dahan River section are part of the south-plunging Tahsi Anticline (Fig. 1), and they have continuous exposures along the river bed of the Dahan River from Neicha to the Shihmen Dam in a stratigraphically up section (i.e. southward) direction (Figs 1b,2). A complete foreland succession in northern Taiwan comprises, from bottom to top, the Kueichulin Formation, the Chinshui Shale, the Cholan Formation, the Yangmei Formation, and the Taomaopu Conglomerate (Fig. 3; Tu & Shao 2001; Lin *et al.* 2003). Because of the aforementioned structural truncations caused by the Taipei Fault at the base and the Hsintien Fault at the top, the studied section does not exhibit a complete foreland succession: the lower part of the Kueichulin Formation (i.e. the base of the foreland succession) and the Taomaopu Conglomerate (i.e. the top of the foreland succession) are absent as a result of fault truncation (Fig. 4). Nonetheless, this section contains the only continuous stratigraphic exposures present in northern Taiwan and provides a record of most of the foreland sedimentary succession; moreover, this section has not been previously studied and documented.

Figure 4 shows that the foreland strata thin westwardly, with the Kueichulin Formation onlapping progressively over the passive margin succession (i.e. atop the Nanchuang Formation) (Yu & Chou 2001; Lin *et al.* 2003). In the Taoyuan and Hsinchu regions, the Kueichulin Formation is divided into the Tapu Formation and the overlying Erhchiu Formation (Fig. 3), which is equivalent to the upper Kueichulin Formation in this study. The Kueichulin Formation consists of very thick, light grey sandstones intercalated with grey mudstones, and it has been interpreted to represent as wave- and storm-dominated shoreface deposits (Hong & Wang 1988; Yu & Teng 1996). The Chinshui Shale mainly comprises very thick, dark grey shale intercalated with thin beds of yellow, very fine- to fine-grained sandstones, and its total thickness reaches approximately 120 m in northern Taiwan. This formation, deposited in offshore environments, indicates that a transient Pliocene deepening event has occurred since the foreland basin was formed (Covey 1984; Chen *et al.* 2001; Nagel *et al.* 2013). The lower Cholan Formation is composed of very fine- to fine-grained sandstones intercalated with grey mudstones, whereas the upper Cholan Formation consists of interbedded very fine-grained sandstones and mudstones.

The Cholan and the Yangmei Formations exhibit similar lithology, and the formation boundary is not clearly defined. Liu (1990) suggested a conglomerate bed at the topmost part of the Cholan Formation as the boundary between the Cholan

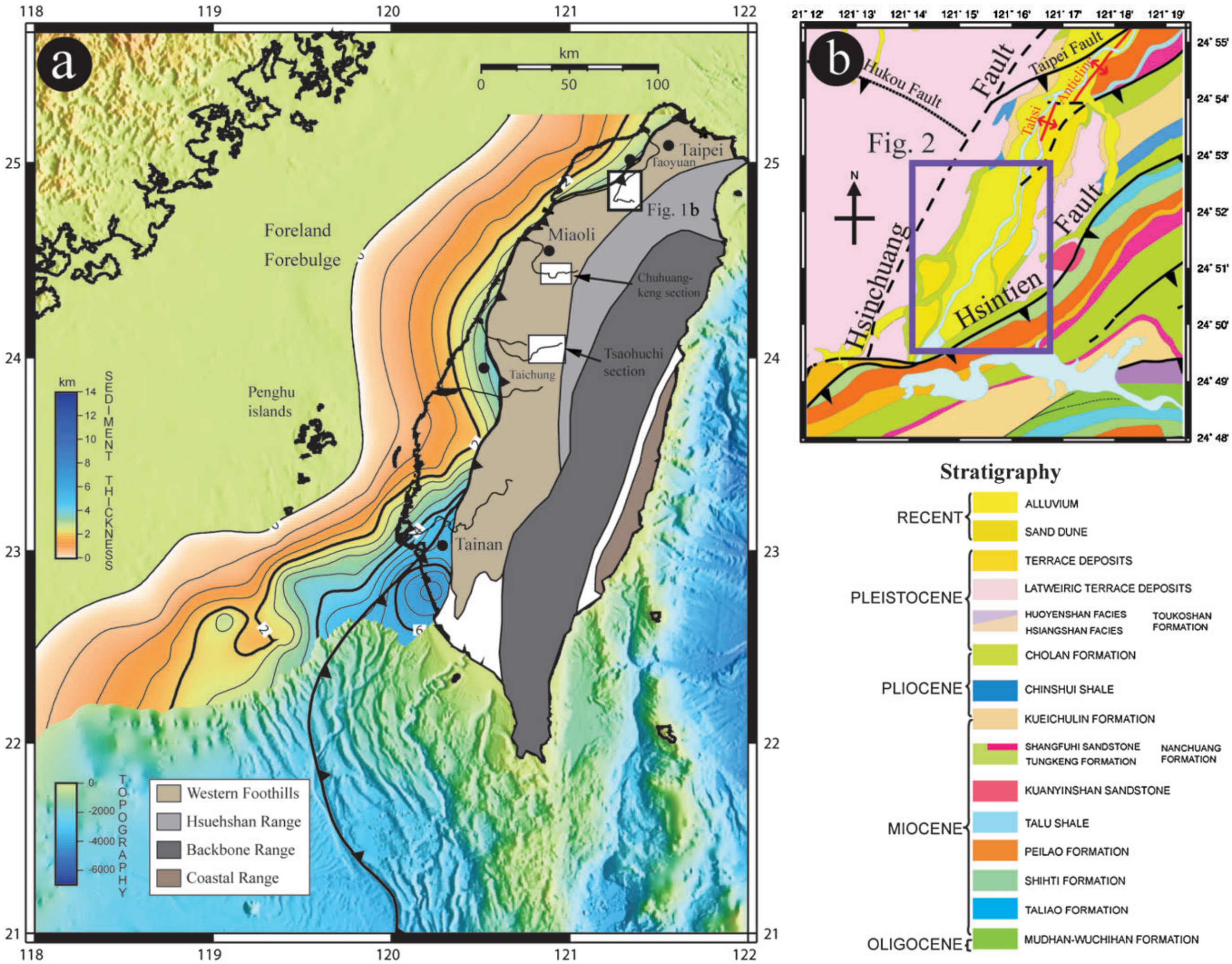

Fig. 1 Geographic and plate-tectonic settings and geological map of NW Taiwan around the studied Dahan River section. (a) Geographic and plate-tectonic settings of Taiwan: a shaded relief map showing the bathymetry and contours to the base of foreland deposits (modified from Lin & Watts, 2002). (b) Geological map of Tahsi and its adjacent area (Chinese Petroleum Corporation, 1978).

and the Toukoushan Formations, and this is equivalent to the Yangmei Formation in the Hsinchu area. In the Dahan River section, no such conglomerate bed exposed and, instead, a 30-m thick, very coarse-grained sandstone layer is present; we infer that this layer is equivalent to the aforementioned conglomerate bed and serves as the boundary between the Cholan Formation and the overlying Yangmei Formation (Fig. 6b).

The Yangmei Formation consists of interbedded very fine-grained sandstones and mudstones, which occasionally intercalated with very coarse-grained sandstones. The Yangmei Formation in the Dahan River section is equivalent to the Chaoching Member of the Yangmei Formation in the Hsinchu area (Tang 1963, 1964) and the Hsiangshan Member of the Toukoushan Formation in central Taiwan (Chang 1955; Ho 1988). The Chaoching Member has been interpreted to be deposits of deltas and meandering rivers, and the Hsiangshan Member has been interpreted to be of braided river origin (Tu & Chen 1984; Chen *et al.* 2001; Huang *et al.* 2002).

Previous biostratigraphic studies in the Miaoli area in NW Taiwan examined the boundary of the Chinshui Shale and Cholan Formation; this boundary coincides with the boundary of the NN15 and NN16 biozones (Huang 1976; Chi & Huang 1981; Chang & Chi 1983), which correspond to the last appearance datum (LAD) of *Reticulofenestra pseudoumbilica*. The age of boundary of the Chinshui Shale and Cholan Formation is 2.43 Ma according to the magnetostratigraphic studies of Chen *et al.* (1977) and Chen *et al.* (2001), with ref-

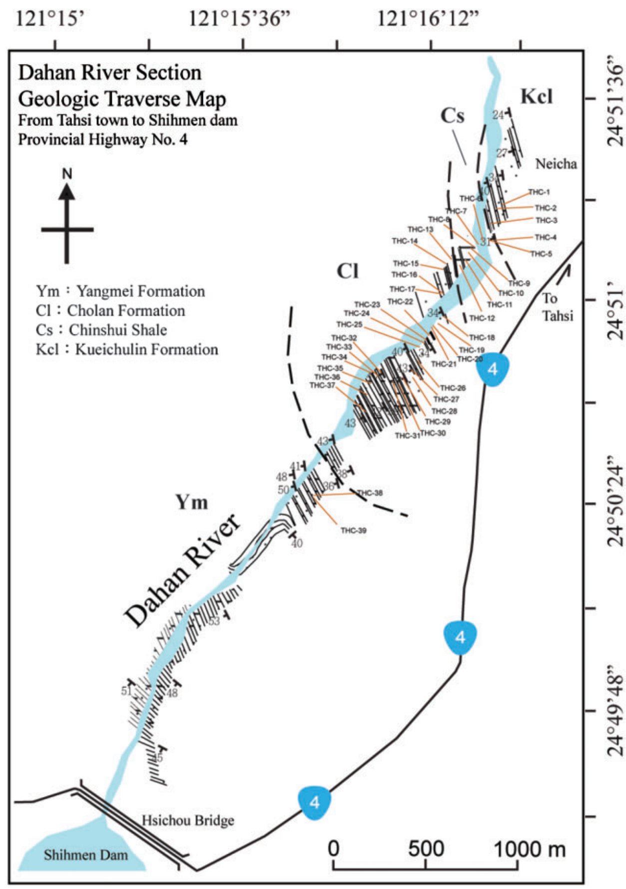

Fig. 2 Geological traverse map of the Dahan River section. The labels THC-01 to THC-39 indicate sampling locations.

erence to the magnetostratigraphic time scale of Cohen and Gibbard (2011). However, Huang and Ting (1981) recommended replacing the LAD of *R. pseudoumbilica* with the LAD of *R. minutulus* as the boundary of the Chinshui Shale and the Cholan Formation. On the basis of this suggestion, recent studies have lowered the NN15/NN16 boundary to make it coincide roughly with the boundary of the Kueichulin Formation and the Chinshui Shale (Shea & Huang 2003; Horng & Shea 2007, see Section 3 for further details). Moreover, the base of the Quaternary Period and the base of Pleistocene Epoch were recently moved from 1.806 to 2.588 Ma (Gibbard & Head 2009); this indicates that the lithostratigraphic boundary of the Chinshui Shale and the Cholan Formation is mostly correlated to the Pliocene–Pleistocene boundary (Fig. 3).

NANNOFOSSIL BIOSTRATIGRAPHY

We collected 39 samples from the strata of Dahan River section (Fig. 2); 3 samples were obtained from the upper Kueichulin Formation (THC-01 to THC-03), 9 were obtained from the Chinshui Shale (THC-04 to THC-12), and 27 were collected from the Cholan Formation (THC-13 to THC-39). No samples were collected from the Yangmei Formation because the sediments of this formation are mostly of nonmarine origin.

Table 1 shows the calcareous nannofossils recognized in the studied samples. We used the zonation scheme of Chang and Chi (1983) to determine the nannofossil biozones of the studied section. Our results show that the samples THC-1 to THC-11 contain nannofossils of *Calcidiscus macintyrei*, *Sphenolithus abies*, *Pseudoumbilica lacunosa*, and *R. pseudoumbilica*, which pertain to the NN15 biozone. The presence of *R. pseudoumbilica* indicates that these samples can be assigned to the NN15 biozone of the early Pliocene age.

For samples THC-12 to THC-20, index fossils of the NN15 zone (e.g. *R. pseudoumbilica* and *S. abies*) were absent. However, these samples contained species of the late Pliocene age, such as *Calcidiscus macintyrei*, *P. lacunosa*, *Crenalithus doronicoides*, *Helicosphaera carteri*, *H. selli*, and *Ceratolithus cristatus*, indicating that samples THC-12 to THC-20 can be assigned to the NN16–NN18 zones. The boundary of NN15 and NN16 coincides roughly with the boundary of the Chinshui Shale and the Cholan Formation. A similar conclusion was also reached in the case of other stratigraphic sections of the Houlungchi section (Chi & Huang 1981) and the Chuhuangkeng section in the Miaoli area in NW Taiwan (Huang 1976; Chang & Chi 1983).

The NN15/NN16 boundary of this study differs from that in the studies of Shea and Huang (2003) and Horng and Shea (2007), in which the NN15/NN16 boundary was placed at the boundary of the Keuichulin Formation and the Chinshui Shale (Fig. 3), with the boundary of the Chinshui Shale and the Cholan Formation coinciding with the LAD of *R. minutulus* (Huang & Ting 1981). The difference arises because of disparity in the size used for recognizing *R. pseudoumbilica*. Shea and Huang (2003) and Horng and Shea (2007) recognized *R. pseudoumbilica* samples that were <5 μm in placolith size as *R. minutulus* (Backman 1978); however, even at this size, we considered the species to be *R. pseudoumbilica*. Thus, Shea and Huang and Horng and Shea concluded that the boundary between the Chinshui Shale and the Cholan Formation should coincide with the LAD of *R. minutulus* rather than with that of *R. pseudoumbilica*.

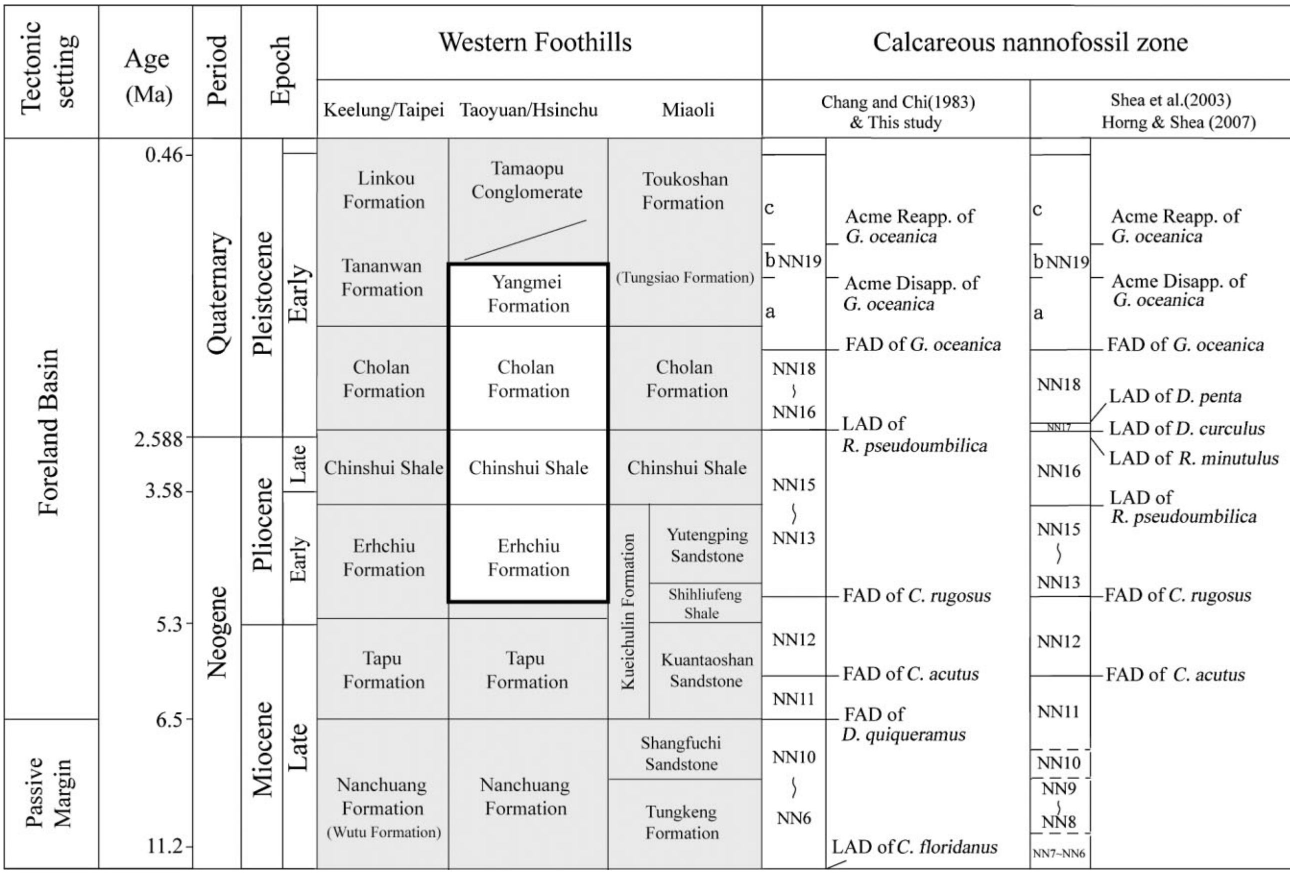

Fig. 3 Late Miocene to Pleistocene stratigraphy in NW foothills, Taiwan. A rectangle indicates the studied formations.

LITHOFACIES, FACIES ASSOCIATIONS AND PALEOENVIRONMENTS

We recognized 17 lithofacies, 2 ichnofacies, and 13 facies associations (FAs) in the Pliocene to Lower Pleistocene series exposed along the Dahan River section. Tables 2–4 summarize the detailed characteristics of each lithofacies, ichnofacies, and FAs and show our interpretations. The stratigraphic column of the Dahan River section (Figs 5, 6) shows vertical arrangements and temporal variations of lithofacies and FAs in the study area. In this section, we summarize our results and describe the temporal evolution of the studied foreland succession in stratigraphic ascending order.

KUEICHULIN FORMATION (UPPER PART, EARLY PLIOCENE)

Lithofacies

The upper part of the Kueichulin Formation (0–140 m of the stratigraphic column shown in Fig. 6a) comprises mostly very fine- to medium-grained sandstones and contains a few mudstone interbeds. One of the common lithofacies is intensely bioturbated sandstone (lithofacies Sb, Table 2), which contains shell fragments, echinoids fossils, coal debris and features, and relict wavy bedding. Other common lithofacies are fine- to medium-grained sandstones exhibiting planar cross-stratifications (Spx), tidal bundles (St), and wavy and flaser bedding (Sw). The commonly observed trace fossils included those of *Rosselia* (Fig. 7a), *Thalassinoides* (Fig. 7b), *Ophiomorpha* (Fig. 7c), *Conichnus* (Fig. 7d), and *Paleophycus*. Lithofacies of slightly bioturbated mudstone (Mb) contains *in situ* crab fossils (Fig. 7e) and shell fragments at the base. Lithofacies of sandstones showing hummocky cross-stratification (Shx) were occasionally detected interbedded with the mudstone.

There are several coarsening-upward successions that are tens of meters thick, and the maximal thickness reaches 30 m. The thickness of these successions decreases upward, and this decrease is coupled with an overall reduction in the

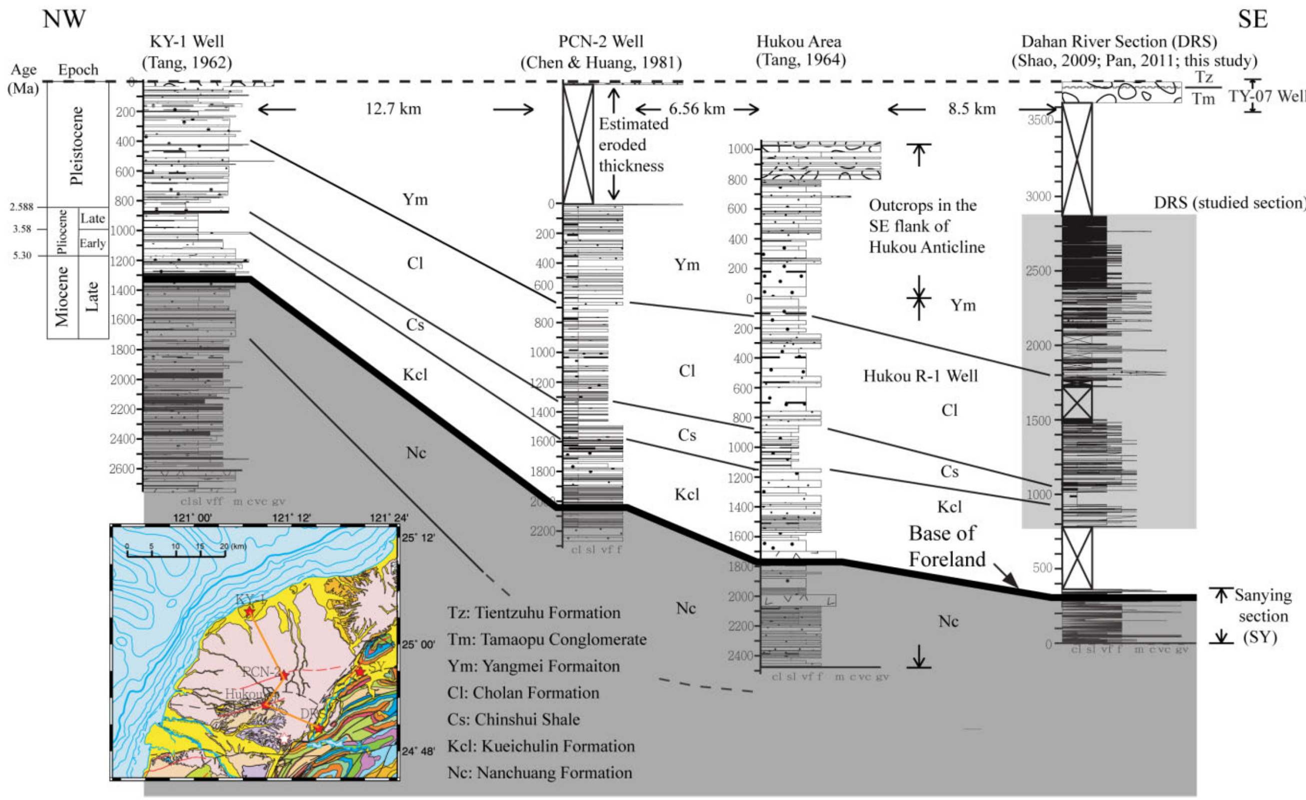

Fig. 4 A foreland stratigraphic correlation in NW Taiwan in the NW–SE direction. The thick solid line represents the base of foreland basin successions and the grey-shaded strata indicate passive-margin succession. The studied formations (shown in the far-right panel) are indicated by a light-grey rectangle. The lower part of the Kueichulin Formation and the Taomaopu Conglomerate are absent because of fault truncation, as detailed in the text.

grain size of each succession, indicating that these successions are arranged in a retrogradational stacking pattern.

Facies associations and paleoenvironments

The upper part of the Kueichulin Formation was interpreted primarily as wave- and tide-influenced open-marine environments, and the FAs (Table 4) included offshore (FA1), lower shoreface (FA2), tidally influenced shoreface (FA3), and tidal inlets/barrier islands (FA4). The occurrence of lithofacies with tidal bundles (St), bipolar paleocurrents (Fig. 6a), and wavy and flaser beddings (Sw) indicates that the sediments are not only accumulated in tide-influenced marine settings but also in wave-influenced settings (e.g. Ghosh *et al.* 2004; Roddaz *et al.* 2006). The presence of hummocky cross-stratified sandstones (Shx) interbedded with bioturbated mudstone (Mb) indicates occasional storm events. The trace-fossil suites of the lower-shoreface FA (FA2) and tidally influenced shoreface (FA3) exhibited proximal *Cruziana* ichnofacies and *Skolithos* ichnofacies, respectively, as determined by referencing the ichnofacies studies of Pemberton *et al.* (2001), MacEachern *et al.* (2007), and Gerard and Bromley (2008). Each coarsening-upward succession represents a shallowing of the environments from offshore to the tide-influenced shoreface. Nevertheless, these shallowing-upward successions thin in the upward direction, and this indicates that the environments in the upper Kueichulin Formation deepened from the shoreface to a deeper offshore marine region.

CHINSHUI SHALE (LATE PLIOCENE)

Lithofacies

The Chinshui Shale is approximately 125 m thick (140–265 m shown in the stratigraphic column of Fig. 6a). The main lithofacies is slightly bioturbated mudstone (Mb), and at the upper part of this formation, thinly bedded and intensely bioturbated sandstone beds (Sb) appear. In the Chinshui Shale, *in situ* fossil crabs and trace fossils of *Teichichnus* (Fig. 7f) were commonly observed.

Table 1 Occurrence of calcareous nannofossils in the studied samples. Sample collection sites and stratigraphic positions are shown in Figs 2 and 6, respectively

Formation	Kueichulin Fm.			Chinshui Shale								Cholan Formation																							
Age	Early Pliocene											Late Pliocene																							
Zonation	NN 15											NN 16																							
Sample Fossils	1	2	3	4	5	6	7	8	9	10	11	12	13	14	15	16	17	18	19	20	21	22	23, 24	25	26	27	28	29	30	31, 32	33	34	35	36	37, 38, 39
Reticulofenestra pseudoumbilica	F	F	F	R	R	R	R	R	VR	R	R		VR	P			P	P	P		P														
Crenalithus doronicoides	F	F	F	A	A	A	C	C	C	C	A		C			R	R	F	F		F	P			R	F	R	R							
Coccolithus pelagicus	F	R	R	R		R	R	R	R	R	R							VR	VR		R	P				R			P						
Reticulofenestra sp.(small)	R	F	F	A	A	C	C	C	C	C	A		C	C	F	VR	R	F	VR	VR			R	R	F	F	R	R		P					
Helicosphaera carteri	P			VR																					P	VR									
Pseudoumbilira lacumosa	P	P	R	VR	R	R	VR	VR	VR	R	R		R	R	F		VR	VR		R	VR			F	F	F	R	R							
Helicosphaera sellii	P	R	F	F		F	F		R	R	R										R			P	R	R									
Calcidiscus macintyrei			P		P						P																								
Sphenolithus abies	P					P	R	P											P	P															
Discolithina		P					P																												
Ceratolithus cristatus	P																									P									
Reticulofenestra pseudoumbilica (large)					R	R	R	R		VR															P								P		
Cyclicargolithus floridanus (reworked)					P	VR	VR				P														P	P	P							P	
Sphenolithus heteromorphus (reworked)						P																													
Gephyrocapsa						P		F			F			R																					
Discoaster sp. / Discoaster asymmetricus							P																												
Helicosphaera ampliaperta / Coccolithus pelagicus										P																					P				

A, abundant; C, common; F, fair; R, rare; VR, very rare; P, 1–2 specimens.

Facies associations and paleoenvironments

The offshore FA (FA1) is predominant in the Chinshui Shale, and the lower-shoreface FA (FA2) occurs only in the upper part of this formation. The appearance of *Teichichnus* indicates that the environment was below the fair-weather wave base and deeper than that at the Kueichulin Formation stage (MacEachern *et al.* 2007). Furthermore, in the entire foreland succession, water was the deepest during the deposition of the Chinshui Shale.

CHOLAN FORMATION (EARLY PLEISTOCENE)

Lithofacies

The boundary between the Chinshui Shale and the Cholan Formation is a gradational contact exhibiting a coarsening-upward trend from slightly bioturbated mudstone (Mb) to intensely bioturbated sandstone (Sb, Fig. 8a). The lower Cholan Formation (265–625 m in the stratigraphic columns of Fig 6a,b) consists of lithofacies of fine-grained sandstone with planar cross-stratification (Spx, Fig. 8b), tidal bundles (St, Fig. 8c), and wavy and flaser bedding (Sw, Fig. 8d,e), which alternate with bioturbated mudstone (Mb) containing shell fragments. Very fine-grained sandstones are intensely bioturbated with trace fossils of *Ophiomorpha*, *Thalassinoides*, *Rosselia*, and *Skolithos*, and the lower part of this formation contains numerous shells and an abundant amount of coal debris (Fig. 8f).

The upper Cholan Formation (625–1023 m in the stratigraphic column of Fig. 6B) comprises mainly very fine- to fine-grained sandstone and mudstone interbeds and occasionally harbors intensely bioturbated sandstone (Sb). Several fining-upward 5–10-m-thick successions are present here, and the common lithofacies are sandstone layers exhibiting wavy bedding (Sw), planar bedding (Sp), planar cross-stratification (Spx), and current ripples (Scr). Moreover, *in situ* tree trunks or rootlets were observed in the mottled mudstones (Mm).

Facies associations and paleoenvironments

We interpreted the lower part of the Cholan Formation to be of wave-dominated estuarine origin, featuring FAs of tidal inlets/barrier islands (FA4), flood deltas (FA5), bay-head deltas (FA6), estuarine central basins (FA7) and tidal flats (FA8). The

Table 2 Summary of identified lithofacies and their interpretation

Lithofacies	Lithology and sedimentary structures	Fossils	Depositional Processes
Ml Parallel-laminated mudstone	Grain size: mud to silt. 0.5–8 m thick bedsets. Parallel lamination.	No visible macrofossils.	Low energy, deposition primarily from suspension.
Mb Bioturbated mudstone	Sandy mudstone. Sand/mud ratio: 1:9 to 2:8. 2–5 m thick bedsets, and tens of meters thick bedsets in Chinshui Shale. Massive, few sedimentary structures.	Echinoids, crabs, and abundant shell fragments.	Low energy environments with lightly to medium bioturbation.
Md Contemporaneously deformed mudstone	Grain size: mud to silt. 1 m thick bedsets. Dewatering structures.	No visible macrofossils.	Sediment loading of water-saturated mud layers.
Mm Mottled mudstone	Grain size: mud. 1–3 m thick bedsets. Massive. Mottled appearance. Greyish-green, black & reddish in color.	*In situ* tree trunk & roots.	Paleosol. Pedogenic processes. weathering & eluviation.
MSw Wavy-bedded sandstone & mudstone interbeds	Grain size: mud to fine sand. Mudstone & sandstone interbeds. 2–7 m thick bedsets. Wavy bedding.	No visible macrofossils.	Alternate of low to high energy traction bed load deposition of sand and flocculated clay. Wavy bedding results from the fluctuation of wave and tidal strength.
Sw Wavy-bedded sandstone	Grain size: fine to medium sand. 0.5–1 m thick bedsets. Flaser and wavy bedding.	Abundant shell fragments & a few plant fragments.	Interspersed of low to high energy traction bed load deposition of sand alternating with flocculated clay. Flaser and wavy bedding results from the fluctuation of wave and tidal strength.
St Tidal bundle cross-stratified sandstone	Grain size: fine to medium sand. 0.5–1 m thick bedsets. Cross-bedding with wavy mud drapes on foresets (tidal bundles). Mudclasts (1–5 cm in diameter).	Shell fragments.	Alternate of low to high energy traction bed load deposition of sand alternating with flocculated clay. The wavy mud drapes on cross bedding foresets result from the fluctuation of tidal strength.
Sp Planar-bedded sandstone	Grain size: fine to medium sand. 0.2–1 m thick bedsets. Well-sorted. Planar bedding.	Abundant shell fragments & a few plant fragments.	High energy plane-bed tractional deposition under unidirectional, oscillatory or combined flows.
Sb Bioturbated sandstone	Muddy sandstone. Sand/mud ratio: 6:4 to 8:2. 2–15 m thick bedsets. Structureless, few relict sedimentary structures.	Abundant echinoids, shell fragments & a few plant fragments.	Low energy environment with intense bioturbation.
Spx Planar cross-stratified sandstone	Grain size: fine to medium sand. 0.5–2 m thick bedsets. Planar cross stratification.	Abundant shell fragments & a few plant fragments.	High energy tractional bed load deposition from uni-directional currents.
Stx Trough cross-stratified sandstone	Grain size: fine to coarse sand. 1–2 m thick bedsets. Trough cross stratification.	Abundant plant fragments.	High energy tractional bed load deposition, usually accumulated in channels.
Shx Hummocky cross-stratified sandstone	Grain size: fine to medium sand. Up to 30 cm thick bedsets. Hummocky cross stratification.	No visible macrofossils.	High energy combined flows in shelf during storms.
Scr Current ripple cross-stratified sandstone	Grain size: very fine to fine sand. 0.2–2 m thick bedsets. Current ripples.	No visible macrofossils.	unidirectional currents.
Scl Climbing ripple cross-stratified sandstone	Grain size: very fine to fine sand. 20–30 cm thick bedsets. Climbing ripples.	No visible macrofossils.	Waves or currents. high concentration of bedload transport.
Sd Contemporaneously deformed Sandstone	Grain size: very fine to fine sand. 0.5–1 m thick bedsets. Ball-and-pillow, load and flame structures.	No visible macrofossils.	Synsedimentary deformation structures by shock (e.g. earthquakes) or rapid deposition of sand over a hydroplastic mud layer.
Sbc Bioclastic sandstone	Grain size: fine to medium sand. 20–30 cm thick bedsets. Structureless. Directly overlying erosional surfaces.	Abundant broken shells & a few plant fragments. Poorly sorted shells are not stratified.	Transgressive lags.
Sm Mud-clast sandstones with rip-up mudstone clasts	Grain size: medium to very coarse sand. 0.5–1 m thick bedsets. Mudclasts (10–20 cm in diameter). Sit directly above an erosional surface.	No visible macrofossils.	Channel lags.

Table 3 Summary of identified ichnofacies and their interpretation

Ichnofacies	Trace fossils	Interpretation	Environments
Skolithos ichnofacies	*Ophiomorpha isp., Planolites isp., Paleophycus isp., Rosselia isp., Conichnus isp., and Skolithos isp.*	Primarily composed of dwelling structures with subordinate deposit-feeding structures	Tidally influenced shoreface, tidal inlets/barrier islands, flood-tidal deltas and bay-head deltas of estuary setting (Pemberton *et al.* 2001; MacEachern *et al.* 2007).
Cruziana ichnofacies	*Ophiomorpha isp., Rosselia isp., Conichnus isp., Planolites isp., Thalassinoides isp., and Teichichnus isp.*	Mainly of dwelling structures with deposit-feeding traces	Lower shoreface and estuarine central basin in estuarine setting (Pemberton *et al.* 2001; MacEachern *et al.* 2007).

thickly bedded sandstone layers exhibiting tidal bundles (St), planar cross-stratification (Spx), and wavy bedding and mudclasts (Sw) were interpreted to be barrier-island/tidal-inlet deposits in a wave- and tide-influenced estuary. The thickly bedded and intensely bioturbated sandstone layers intercalated with barrier-island/tidal-inlet deposits were interpreted to be estuarine central-basin deposits, which are accumulated in a low-energy environment protected by barrier islands; this interpretation is consistent with those of Gingras *et al.* (2002) and Abdel-Fattah *et al.* (2010). The molluscs and coal debris overlying erosional surfaces were interpreted to be a part of the lag deposits formed during marine transgression (c.f. Catuneanu 2006). The FAs of tidal inlets/barrier islands (FA4) and bay-head deltas (FA6) were associated with trace-fossil suites of *Skolithos* ichnofacies, whereas the estuarine central-basin FA (FA7) was associated with *Cruziana* ichnofacies (c.f. Pemberton *et al.* 2001; MacEachern *et al.* 2007; Gerard & Bromley 2008).

We concluded that the sediments of the upper Cholan Formation accumulate at the margins of estuaries, in the transition zones between estuaries and fluvial environments. The FAs include estuarine central basins (FA7), tidal flats (FA8), fluvial channel bars (FA9), crevasse splays (FA10), levees (FA11), and flood plains (FA12). The sandstone layers of the fining-upward successions exhibit planar bedding (Sp), planar cross-stratification (Spx), and current ripples (Scr), which represent channel bars and levee deposits, whereas the mudstone layers containing *in situ* tree trunks or rootlets indicate flood-plain deposits. The environments evolved from coastal settings in the lower Cholan Formation to fluvial systems in the upper Cholan Formation, and this indicates an overall shoaling-upward trend of the infilling foreland stratigraphy.

YANGMEI FORMATION (EARLY PLEISTOCENE)

Lithofacies

The Yangmei Formation (1023–2094 m in the stratigraphic column of Figs 6b to 6d) mainly comprises lithofacies of well sorted, very fine- to fine-grained sandstone with planar bedding (Sp), planar cross-stratification (Spx), current ripples (Scr, Fig. 9a), climbing ripples (Scl), and loading structures (Sd), which intercalated with slightly mottled mudstone (Mm) containing *in situ* rootlets or tree trunks (Fig. 9b,c) and small amounts of tooth fossils of mammals. This formation occasionally intercalated with lithofacies of medium- to very coarse-grained and poorly sorted sandstones exhibiting trough cross-stratification (Stx), mudclasts overlying erosional surfaces (Sm, Fig. 9d), and coal debris (Fig. 9e). The vertical arrangement of the lithofacies showed a fining-upward trend (i.e. a succession) 5–15 m in thickness (Fig. 9f). These successions disappear at upper part of the stratigraphic column, and the thickness of the sandstone or mudstone layers decreases to 1–3 m each, representing an overall thinning and fining-upward trend.

Facies associations and paleoenvironments

The sediments of the Yangmei Formation were interpreted to accumulate in meandering and sandy braided rivers. The FAs (Table 4) include fluvial channel bars (FA9), crevasse splays (FA10), levees (FA11), flood plains (FA12), and sandy braided river deposits (FA13). The thickly bedded,

Table 4 Summary of interpreted facies associations

Facies Association	Lithofacies	Characteristics	Ichnology/fossil content	Interpretation
FA1: Offshore	Ml, Mb, Shx, Sbc	Primarily composed of mudstones and siltstones. 2 to 10 m thick succession. Tens of meters thick in Chinshui Shale.	Slight bioturbation (BI = 0 to 2). Crabs fossils: *Galene granulifera* and *Charybdis minuta*. Trace fossils: *Teichichnus*. Bivalves fragments.	Below fair-weather wave base (Walker & Plint 1992; Clifton 2006). Low energy, deposition from suspension. Hummocky cross stratification indicates occasional storm events.
FA2: Lower shoreface	Mb, Sb, Sbc	Bioturbated mudstones and sandstones. 3 to 10 m thick succession, occasionally up to 20 m thick.	Intense bioturbation (BI = 5 to 6). Echinoids fossils. Trace fossils: *Ophiomorpha*, *Rosselia*, *Conichinus*, and *Thalassinoides*, representing proximal *Cruziana* ichnofacies (Pemberton *et al.* 2001). Bivalves fragments.	Above fair-weather wave base (Walker & Plint 1992; Reading & Collinson 1996; Clifton 2006). Strong bioturbation indicates relatively low energy environments.
FA3: Tidally influenced shoreface	Spx, Sw, St	Very fine- to fine-grained sandstones. 15 to 25 m thick succession.	Medium bioturbation (BI = 3). Trace fossils: *Ophiomorpha*, *Paleophycus*, and *Rosselia*, represented *Skolithos* ichnofacies.	Above fair-weather wave base and below the mean water level (Reading & Collinson 1996; Clifton 2006). Tidal bundles and mudclasts represented alternating energy of tidal environments (Ghosh *et al.* 2004; Roddaz *et al.* 2006). Wavy and flaser beddings formed in slack-water period of waves and tidal strength. Compared to the paleocurrents of lower shoreface, indicating the effects of bottom oscillatory currents (Clifton 2006).
FA4: Tidal inlet/ barrier island	Sw, St, Spx, Stx, Sf	Very fine- to fine-grained sandstones. 1 to 4 m thick succession, occasionally up to 10 to 15 m in thickness.	Medium bioturbation (BI = 3). Trace fossils: *Ophiomorpha*, *Rosselia*, *Conichinus*, *Planolites*, and *Paleophycus*, represented *Skolithos* ichnofacies. Coal debris.	The opening of the estuarine environments dominated by high energy flows, and influenced by tidal and waves strength.
FA5: Flood-tidal delta	Sw, Spx, Stx, Sbc	Fine-grained sandstones. 10 to 20 m thick succession, coarsening-upward sequence.	Moderate bioturbation (BI = 3). Trace fossils: *Ophiomorpha* and *Skolithos*. Coal debris.	Sediments accumulation at the landward end of the tidal inlets. Plant fragments represented FA5 closed to the margin of the estuaries.
FA6: Bay-head delta	Sw, Spx	Fine-grained yellowish sandstones. 15 m thick succession, coarsening-upward sequence.	Moderate bioturbation (BI = 5). Trace fossils: *Ophiomorpha*, *Planolites*, and *Paleophycus*, represented *Skolithos* ichnofacies. Coal debris.	Sediments accumulation at the head of the estuaries which connected fluvial environments and central basin of the estuaries. Yellowish sandstone beds and coal debris indicated FA6 closed to the margin of the estuaries, which influenced by tide and wave strength.
FA7: Estuarine central basin	Mb, Sw, Sb, Shx, Sd, Sbc	mudstone and very fine- to fine-grained sandstones. 5 to 8 m thick succession, occasionally up to 15 m in thickness.	Slight to strong bioturbation (BI = 1 to 5). Trace fossils: *Planolites*, *Paleophycus*, *Ophiomorpha*, *Thalassinoides*, and *Teichichnus*, represented *Cruziana* ichnofacies. Abundant bivalve and Coal debris.	Inside the barrier island, quiescent bay deposits, occasionally had storm events. Intense bioturbation indicated the relatively low energy environments (Reinson 1992; Abdel-Fattah *et al.* 2010). Sbc lithofacies were transgressive deposits which overlaid on the transgressive ravinement surfaces scoured by tides and waves (Catuneanu 2006).
FA8: Tidal flats	Mm, MSw, Sw, Sp, Spx	Mudstones and very fine-grained sandstones. 3 to 5 m thick succession, fining-upward sequence.	None to moderate bioturbation (BI = 0 to 4). Rootlets.	Located at the margin of the estuaries. Recognized as subtidal and intertidal zone (Boggs 2006; Boyd *et al.* 2006). Subtidal zone was subjected to high tidal-currents velocity producing tidal channels.
FA9: Fluvial Channel bar	Sp, Spx, Stx, Sm	Fine- to very coarse-grained sandstones. 10 to 15 m thick succession. Poorly sorted. Fining-upward sequence. Basal surfaces are erosional.	No bioturbation (BI = 0). Abundant coal debris.	Channel deposits of meandering river systems. High energy currents scoured the bottom and deposited the channel lags.
FA10: Crevasse splay	Ml, Scr, Sd	Mudstone and very fine- to fine-grained sandstone interbeds. 1 to 5 m thick succession	None to slight bioturbation (BI = 0 to 1). Rootlets and tree trunks.	Overbank deposits of meandering river systems. Floodwaters breached the levees intermittently and overlay the floodplain deposits (Collinson 1996).
FA11: Levee	Sp, Scr, Scl	Very fine-grained sandstones. 1 to 2 m thick succession. Fining-upward sequence.	No bioturbation (BI = 0).	Proximal overbank deposits offluvial systems, developed between the channels and the adjacent floodplains (Collinson 1996).
FA12: Flood plain	Ml, Mm	2 to 5 m thick succession.	None to slight bioturbation (BI = 0 to 1). Rootlets and tree trunks.	Distal overbank deposits of fluvial systems. Non-steady rates of sedimentation caused of the compound paleosols with low-maturity (Kraus 1999). Soils with low-permeability or rapidly lateral migration of fluvial channels resulted in absence of rootlets and tree trunks (Ghazi & Mountney 2009).
FA13: Sandy braided river	Ml, Mm, Scr	1 to 3 m thick sandstone and 1 to 2 m thick mudstone interbeds. Sand/mud ratio: 3:1 to 1:1.	None to medium bioturbation (BI = 0 to 4). Coal debris and tree trunks.	Frequently lateral migration of fluvial channels. The channel deposits were covered and stacked with overbank and other channel deposits (Collinson 1996; Nichols 2009).

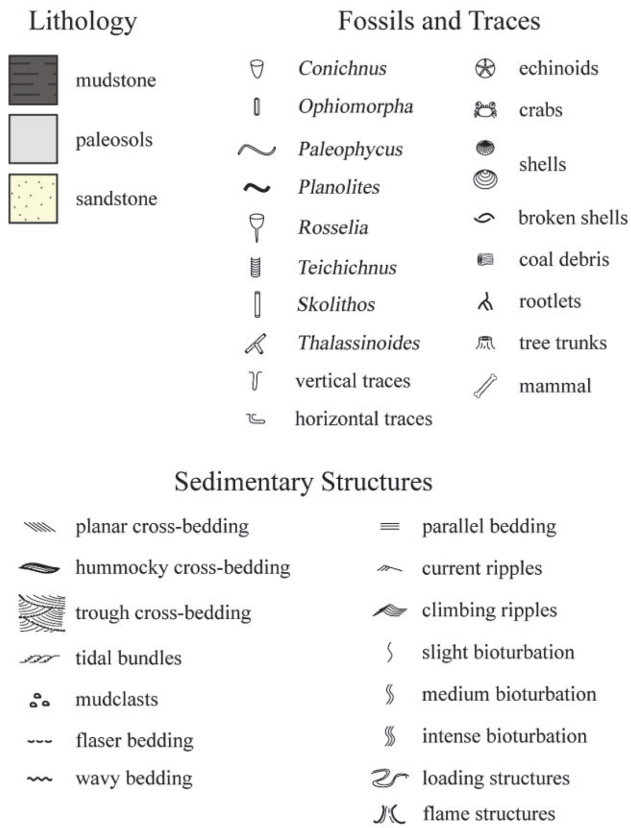

Fig. 5 Legend for symbols used in Figure 6.

medium- to very coarse-grained lithofacies of sandstones detected in the fining-upward successions represent channel-bar deposits (FA9); conversely, overbank deposits (FA10, FA11, and FA12) are represented by the lithofacies of sandstones exhibiting planar bedding (Sp), planar cross-stratification (Spx), current ripples (Scr), climbing ripples (Scl), and loading structures (Sd) intercalated with partly mottled mudstone (Mm) containing abundant plant fragments and *in situ* plants. Here, channel deposits are overlain by overbank and other channel deposits, indicating that the sandy braided river environment (FA13) is characterized by frequent lateral migration of fluvial channels (e.g. Collinson 1996; Nichols 2009).

DEPOSITIONAL SETTINGS

Our analyses of lithofacies, ichnofacies, FAs, and characteristic body fossils revealed that three major sedimentary environments were represented in the studied section (Fig. 10): (i) wave- and tide-influenced open-marine settings; (ii) wave-dominated estuaries; and (iii) meandering and sandy braided river systems.

The wave- and tide-influenced open-marine systems, which include the FAs of offshore (FA1), lower shoreface (FA2), and tidally influenced shoreface (FA3), were recognized in the Kueichulin Formation and in the Chinshui Shale (Fig. 10a). In these strata, the sandstone layers are characterized by planar cross-stratification (Spx), wavy bedding (Sw), tidal bundles (St), and rare hummocky cross stratification (Shx), which indicate the effects of tides and waves and the occurrence of infrequent storm events. Furthermore, the marine beds contain shallow marine fossils such as those of crabs, echinoids, and shells (Sbc) together with ichnofacies of *Skolithos* and *Cruziana*.

In the lower Cholan Formation, we detected wave-dominated estuary systems featuring FAs of tidal inlets/barrier islands (FA4), flood-tidal deltas (FA5), bay-head deltas (FA6), estuarine central basins (FA7), and tidal flats (FA8). The strata contain shallow marine fossils (Sbc) and exhibit *Skolithos* and *Cruziana* ichnofacies. The sandstone layers are characterized by planar cross-stratification (Spx), trough cross stratification (Stx), tidal bundles (St), wavy bedding (Sw), and planar stratification (Sp), indicating tidal and wave influences. However, the presence of sandstone layers abundant in coal debris and lithofacies with wavy-bedded sandstone and mudstone interbeds (MSw) indicate that the systems are situated at the margin of estuaries and transition zones of coastal and fluvial systems (e.g., Reinson 1992; Boyd *et al.* 2006)

In the upper Cholan Formation and the Yangmei Formation, we observe meandering and sandy braided river systems featuring FAs of fluvial channel bars (FA9), crevasse splays (FA10), levees (FA11), flood plains (FA12) and sandy braided rivers (FA13). The appearance of coal debris, rootlets and *in situ* tree trunks, and mottled mudstone (Mm) is a key characteristic of fluvial settings. The thick successions of fine to very-coarse grained sandstone exhibiting planar bedding (Sp), planar cross-stratification (Spx), trough cross-stratification (Stx), and erosional surfaces at the bottom were interpreted to be channel-bar deposits (FA9). Moreover, sandstone and mudstone interbeds characterized by current ripples (Scr), climbing ripples (Scl), planar stratifications (Sp), and contemporaneously deformed structures (Sd & Md) were interpreted to be overbank deposits (FA10, FA11, & FA12). Lastly, we recognized repeated fining-upward successions and channel fills that intercalated with overbank deposits.

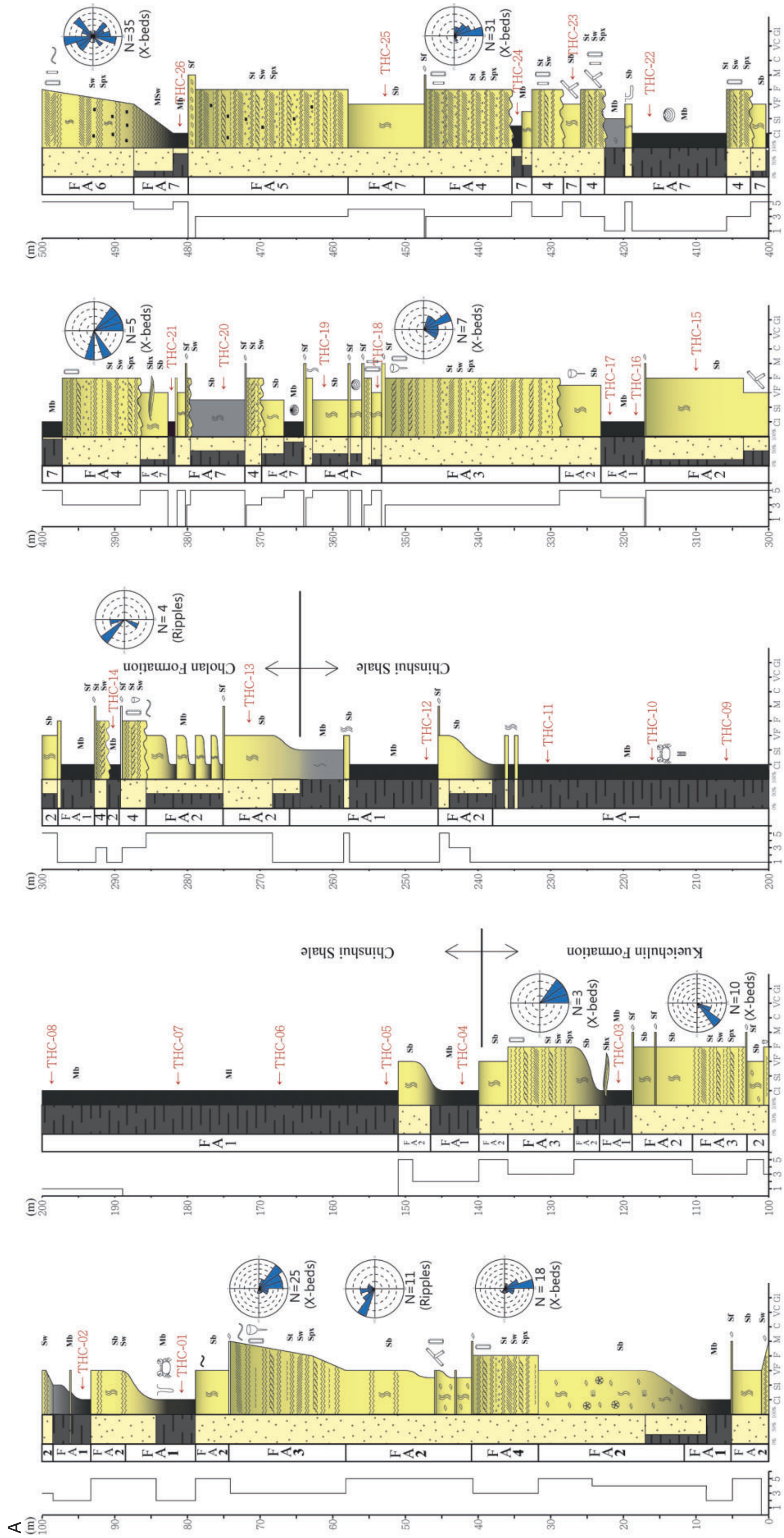

Fig. 6 Stratigraphical/sedimentological columnar sections of the Dahan River section. The degree of bioturbation (bioturbation index, 0–5) is shown on the left and the directions of paleocurrents as shown on the right, alongside the stratigraphic column. (a) 0–500 m; (b) 500–1200 m; (c) 1200–1700 m; (d) 1700–2100 m. The symbols are defined in Figure 5 and the locations are shown in Figure 1.

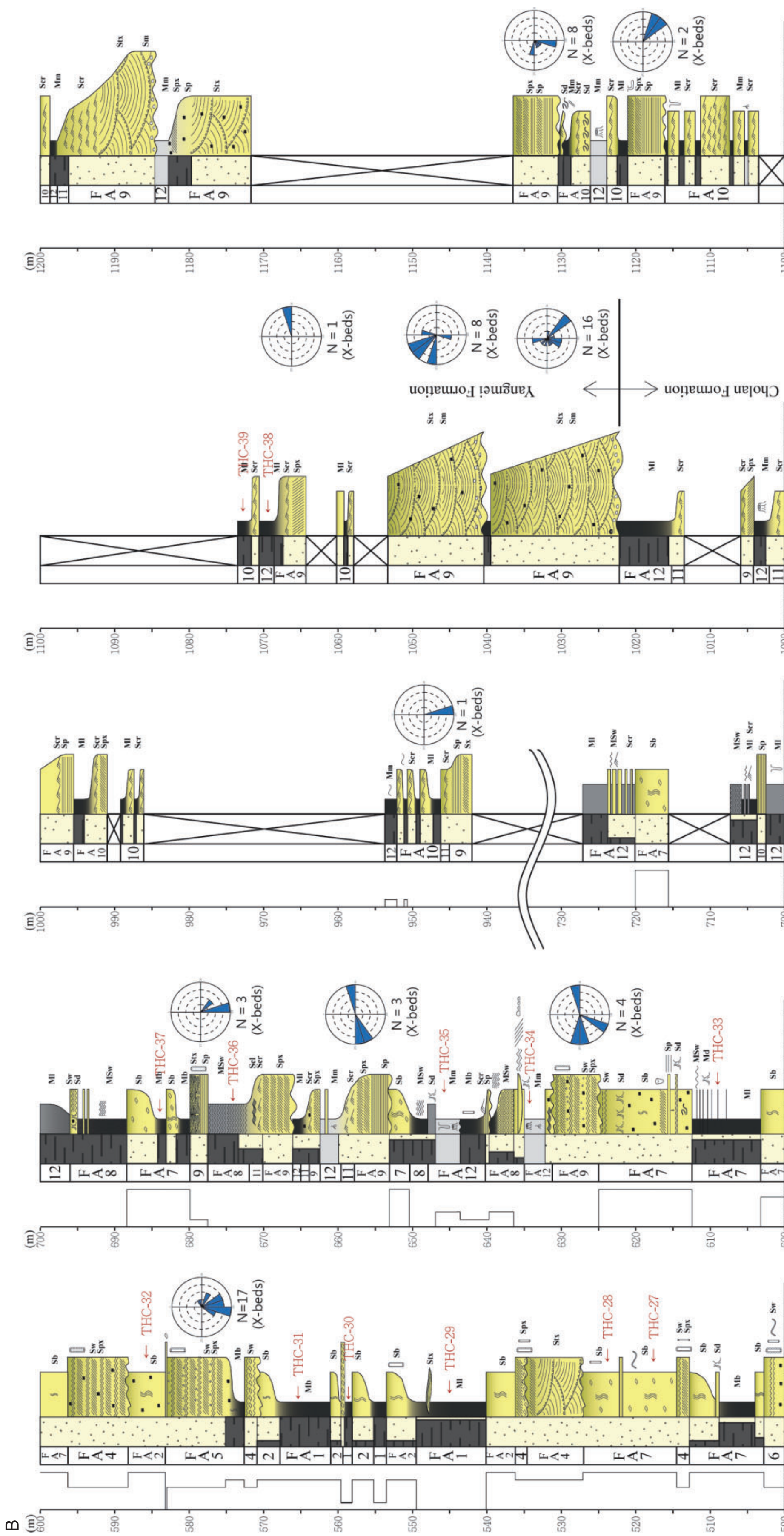

Fig. 6 *Continued*

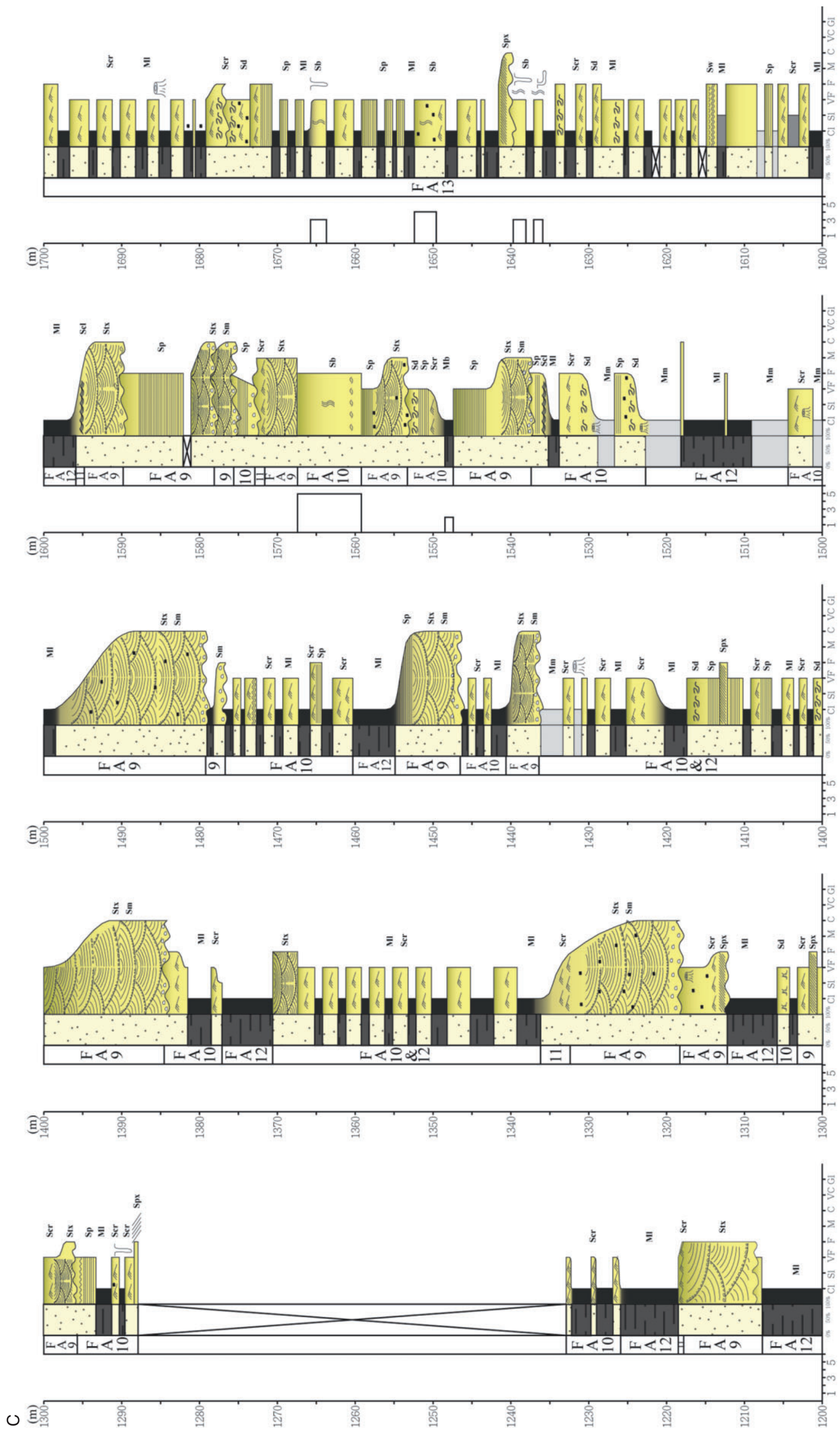

Fig. 6 *Continued*

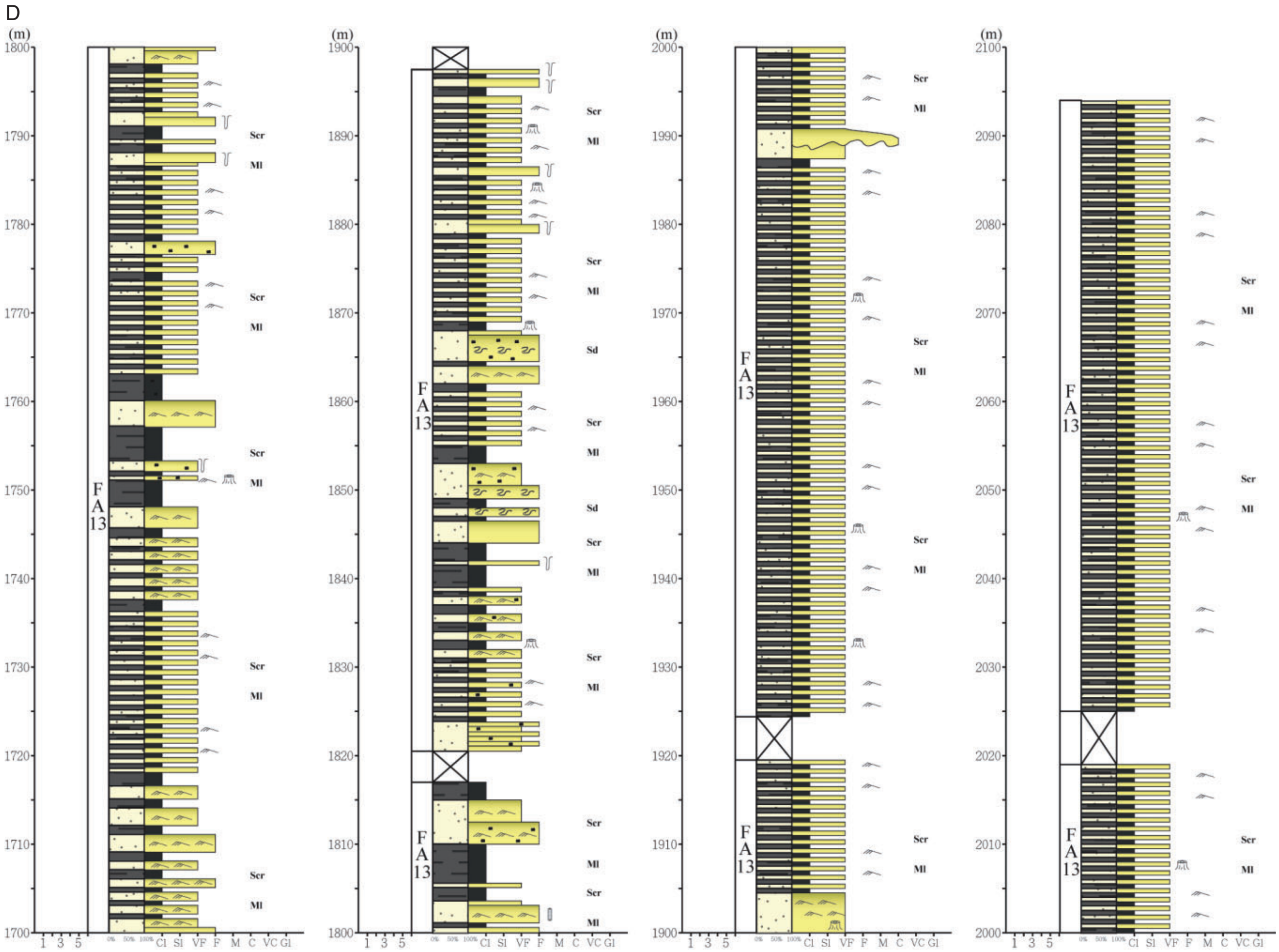

Fig. 6 *Continued*

DISCUSSION

TEMPORAL EVOLUTION OF THE FILLING OF THE FORELAND BASIN IN NORTHWESTERN TAIWAN

The Dahan River section represents a rapidly accumulating foreland basin containing 2100 m-thick sediments deposited during the period of approximately 4–1 Ma, indicating that this basin has exhibited rapid subsidence within approximately 3 my. These deposits reflect the competing effects of the rates of sediment supply and basin subsidence and the studied succession shows that the basin evolved from underfilled to overfilled stages, as described by Covey (1986) (Fig. 11).

Sediments of the early Pliocene in the upper Kueichulin Formation were accumulated in a wave- and tide-influenced shallow marine environment, and this formation represents the deposits of the initial stage of the Taiwan foreland basin (Teng 1990; Lin *et al.* 2003). The northern portion of the Taiwan mountain belt arose during the early Pliocene, and the geotectonic position of this shallow marine environment has been interpreted to be located at the fringe of a foreland adjacent to the forebulge (Lin *et al.* 2003) containing sediments originating from China (Chi & Huang, 1981).

In the late Pliocene and during the deposition of the Chinshui Shale, Taiwan experienced a phase of drastic arc–continent collision as evidenced by accelerated basin subsidence (Chou *et al.* 1994; Lin *et al.* 2003) and rapid orogenic exhumation (Liu *et al.* 2000, 2001; Fuller *et al.* 2006). Frontal accretion and structural underplating of the orogenic belts enhanced the rapid uplift and intense erosion of the orogen (Simoes & Avouac 2006; Beyssac *et al.* 2007; Simoes *et al.* 2007). Rapid exhumation of the Taiwan orogeny increased the amount of loading and thus increased the flexural subsidence of the foreland, deepening the accommodation

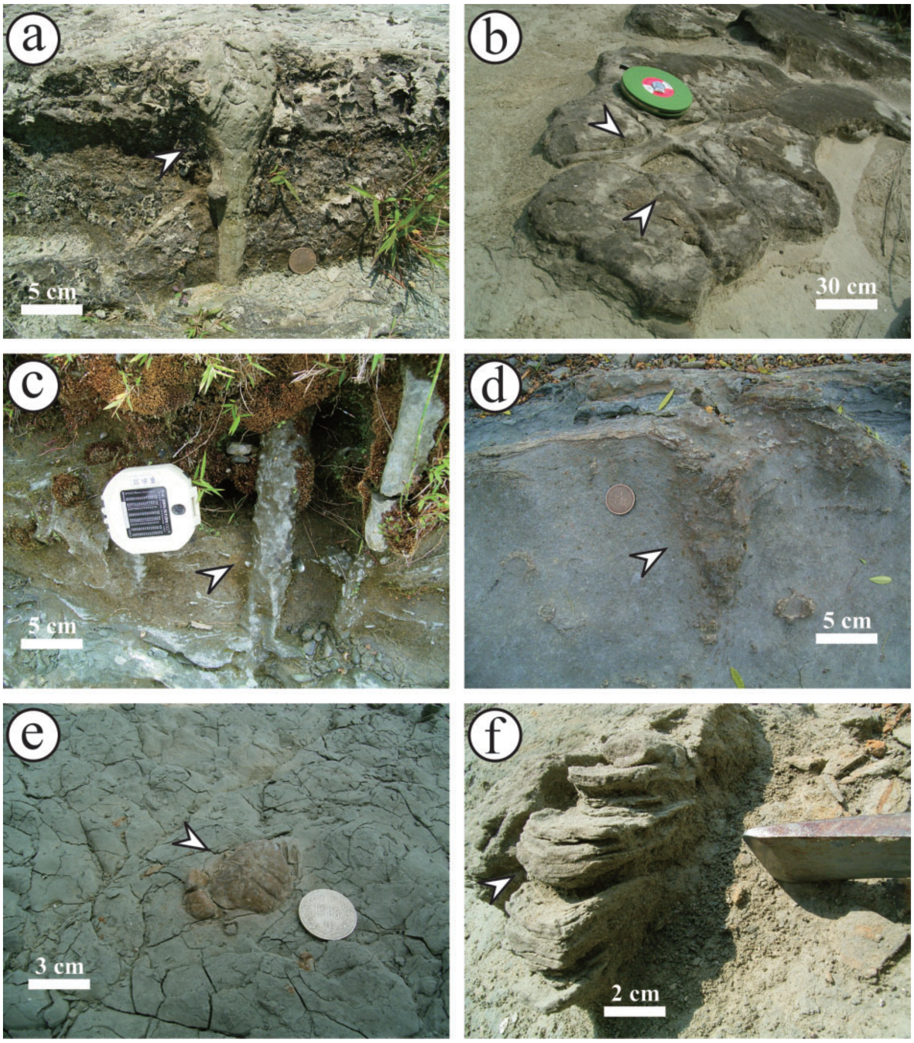

Fig. 7 Trace and body fossils detected in the studied succession. (a) *Rosselia* isp., (b) *Thalassinoides* isp., (c) *Ophiomorpha* isp., (d) *Conichnus* isp., (e) *Galene granulifera* Crab fossils, and (f) *Teichichnus* isp.

space and causing the foreland to become an offshore marine environment (Fig. 11b) (Teng 1987; Chou *et al.* 1994; Lin *et al.* 2003). The Chinshui Shale stage was the deepest environment in the studied foreland succession. The main sediment source changed from China in the west to Taiwan Island in the east (Chi & Huang 1981; Chang & Chi 1983; Chen *et al.*, 1999; Nagel *et al.* 2014) (Fig. 11d,e). The deepening event is considered not to have been controlled by eustatic sea-level changes but to have been of tectonic origin. This interpretation is further supported by the findings that the eustatic sea level was nearly unchanged while the paleoenvironment deepened during the deposition of the Chinshui Shale (Fig. 11a).

At the beginning of the early Pleistocene (approximately 2.5 Ma), the orogen was exhumed more rapidly, and this resulted in an increase of sediment supply (Chen *et al.* 1977; Chi & Huang 1981; Chang & Chi 1983; Simoes *et al.* 2007) (Fig. 11c). The subsequent thick and aggradational successions developed in response to rapid basin subsidence occurring in conjunction with high sediment flux adjacent to the actively eroding orogen. When the sediments of the lower Cholan Formation accumulated, the rate of basin subsidence was almost matched by the rate of sediment supply, and this resulted in an aggradational coastal-sediment package approximately 450 m in thickness. The environments became shallower, transforming from offshore marine environments to wave-dominated estuaries. In the upper Cholan and Yangmei Formation stages, sediment supply outpaced basin subsidence, and this caused the foreland to become a meandering and sandy braided river environment characterized by a coarsening-upward sediment succession of roughly 1200 m.

In summary, the trend of the environmental evolution for the studied succession shows a

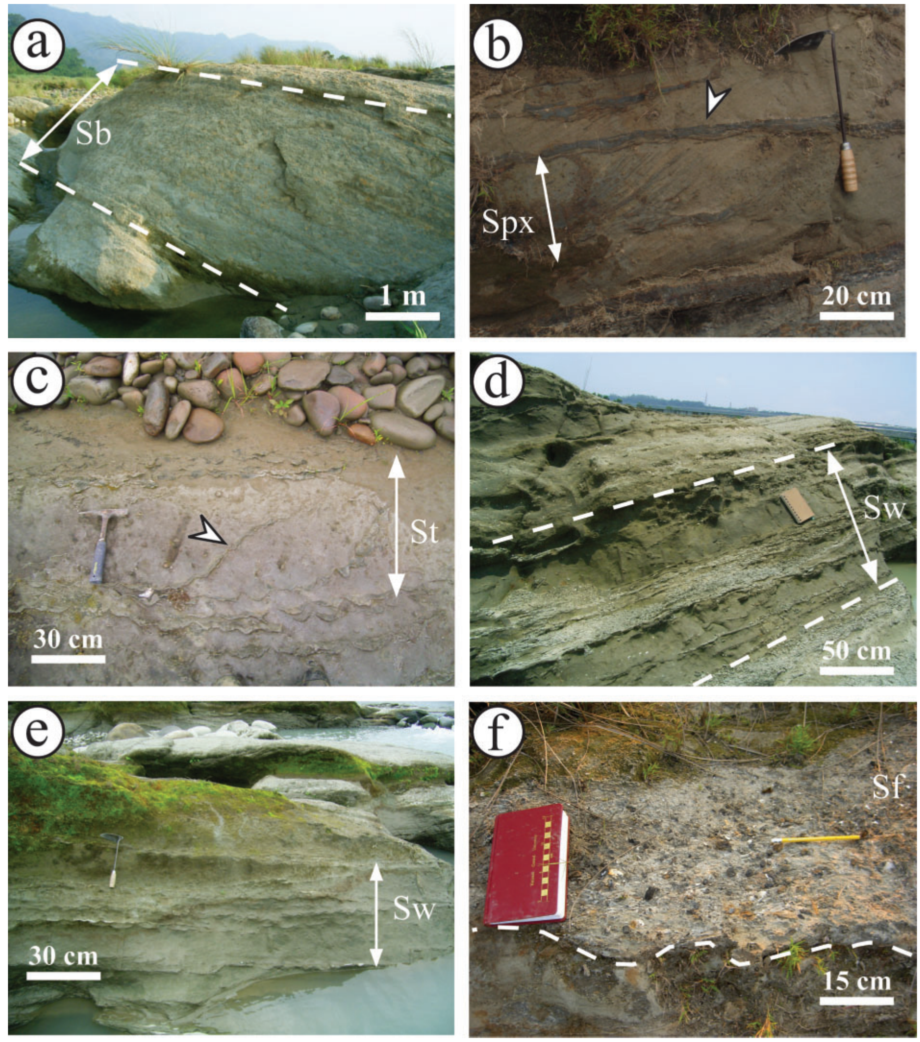

Fig. 8 Lithofacies accumulated in wave- and tide-influenced shallow marine and coastal settings of the Cholan Formation. (a) Intensely bioturbated sandstone (Sb); (b) a sandstone layer exhibiting planar cross-stratification (Spx) and mud drapes (white arrow), indicating varying tidal influences; (c) tidal bundle cross-stratified sandstone (St) containing wavy mud drapes on foresets of cross-stratification (white arrow); (d) wavy-bedded sandstone (Sw) containing mudclasts; (e) wavy-bedded sandstone (Sw) showing flaser bedding; (f) transgressive lags (Sbc) containing shell and coal debris and floored by an erosional surface (indicated by a white dashed line).

deepening from shallow marine to offshore marine settings, followed by a shallowing upward from offshore to fluvial environments during the Pliocene to the Pleistocene age during approximately 4–1 Ma (Fig. 11). The Himalayan foreland basin experienced similar underfilled to overfilled depositional stages (DeCelles *et al.* 1998; Ding *et al.* 2005; Najman *et al.* 2009), with the underfilled stage occurring during 65–42 Ma and leading to a nearly 700-m-thick accumulation of marine sediment. After a 20–15-myr stratigraphic hiatus, fluvial sedimentation resumed during 13–5 Ma in an overfilled stage and led to a > 3000-m-thick sediment accumulation. Compared to the long-lasting underfilled to overfilled depositional stages of the Himalayan foreland basin, the evolution from an underfilled to an overfilled sedimentary state occurring within approximately 3 my in the Taiwan foreland basin involved considerably high rates of basin subsidence and sediment accumulation, reflecting the highly active and short-lived nature of arc-continent collisions.

STRATIGRAPHIC ARCHITECTURE OF THE FORELAND BASIN IN NORTHWESTERN TAIWAN

Here, we show that the foreland basin in NW Taiwan exhibits an along-strike stratigraphic architecture by correlating the northernmost Dahan River section to two representative sections, namely the Chuhuangkeng section and Tsaohuchi section (Fig. 1a) in central Taiwan (Fig. 12). All of these successions exhibit an early deepening trend from shallow marine to offshore marine environments (i.e. from the deposition of the Kueichulin Formation to that of the Chinshui Shale), and a subsequent shallowing upward succession from offshore marine to fluvial

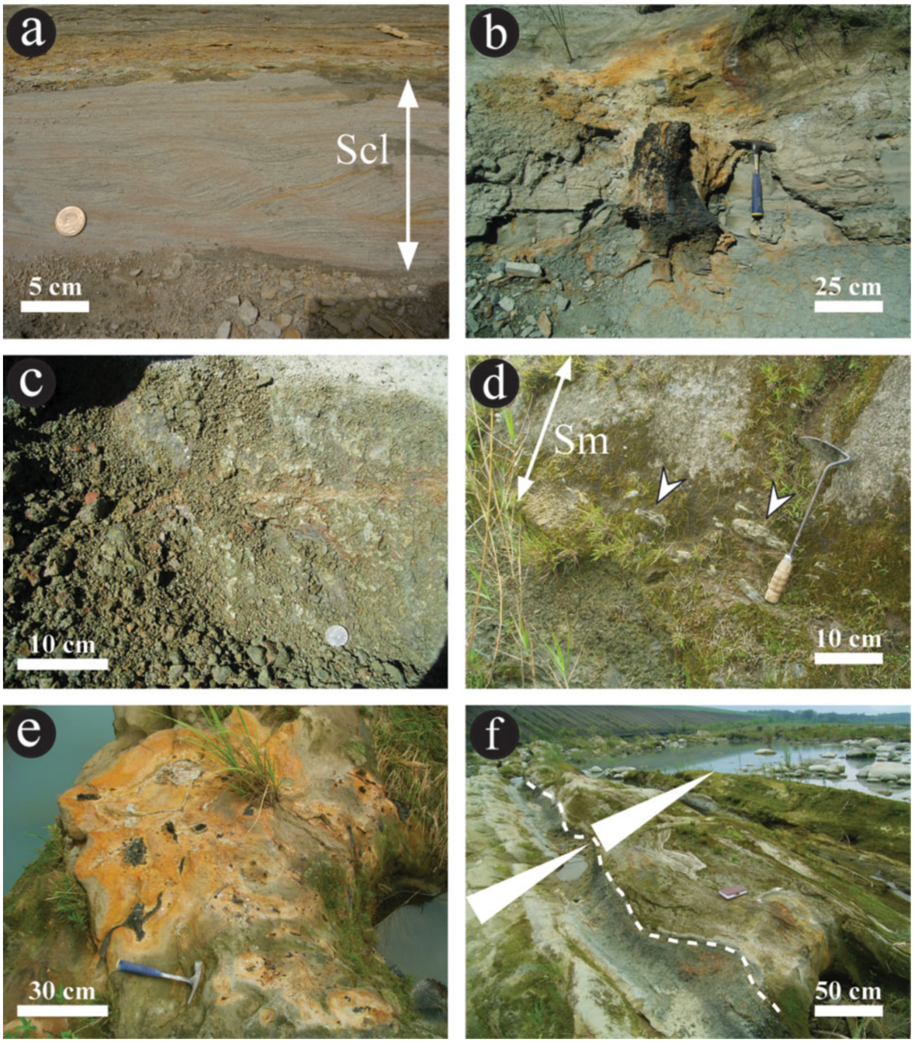

Fig. 9 Meandering and sandy braided river deposits of the Yangmei Formation. (a) Climbing ripple cross-stratified sandstone (Scr); (b) an *in situ* tree trunk; (c) mottled mudstone of various colors (black and red, Sm); (d) mudclast-bearing sandstone (Sm). Mudclasts at the bottom of channel deposits are channel lags (white arrows); (e) Sandstone layers harboring coal debris; (f) erosional contact between 2 fining-upward successions. Strata above the erosion surface (indicated by the white dashed line) are channel deposits, strata below are floodplain deposits.

environments. The trend reveals that the rapid exhumation of Taiwan orogen increased the amount of loading and flexural subsidence of the foreland, and this deepening event occurred contemporaneously along-strike the entire foreland basin during the Chinshui Shale stage. Therefore, we conclude that this deepening event tends to exert a local influence, which is unlikely to represent a signature of a reduction in sediment supply. This mechanism differs from that responsible for the Oligocene to Miocene deposits of the North Alpine Foreland Basin, which represent repeated underfilled to overfilled successions caused by strong collision and a reduction in sediment discharge (Kuhlemann & Kempf 2002).

The northernmost Dahan River section deposited approximately 400 m of shallow marine sediments overlain by fluvial sediments; by contrast, the Chuhuangkeng and Tsaohuchi sections in central Taiwan began to deposit fluvial sediments after accumulating shallow marine sediments that were 1500 and 2400 m thick, respectively (Fig. 12). If the sediment-supply rate is constant, we can attribute the distinct thicknesses of the shallow marine sediments in northern and central Taiwan foreland basin to dissimilar basin subsidence rates. This is evidenced by the amount of foreland subsidence being higher in central Taiwan than in northern Taiwan, as shown in the foreland sediment isopachs (Fig. 1), which exhibit thicker sediments in central Taiwan and near the Tsaohuchi section (Fig. 1a) than in northern Taiwan.

CONCLUSIONS

This study documents the lithofacies, FAs, calcareous nannofossil biostratigraphic zones, and

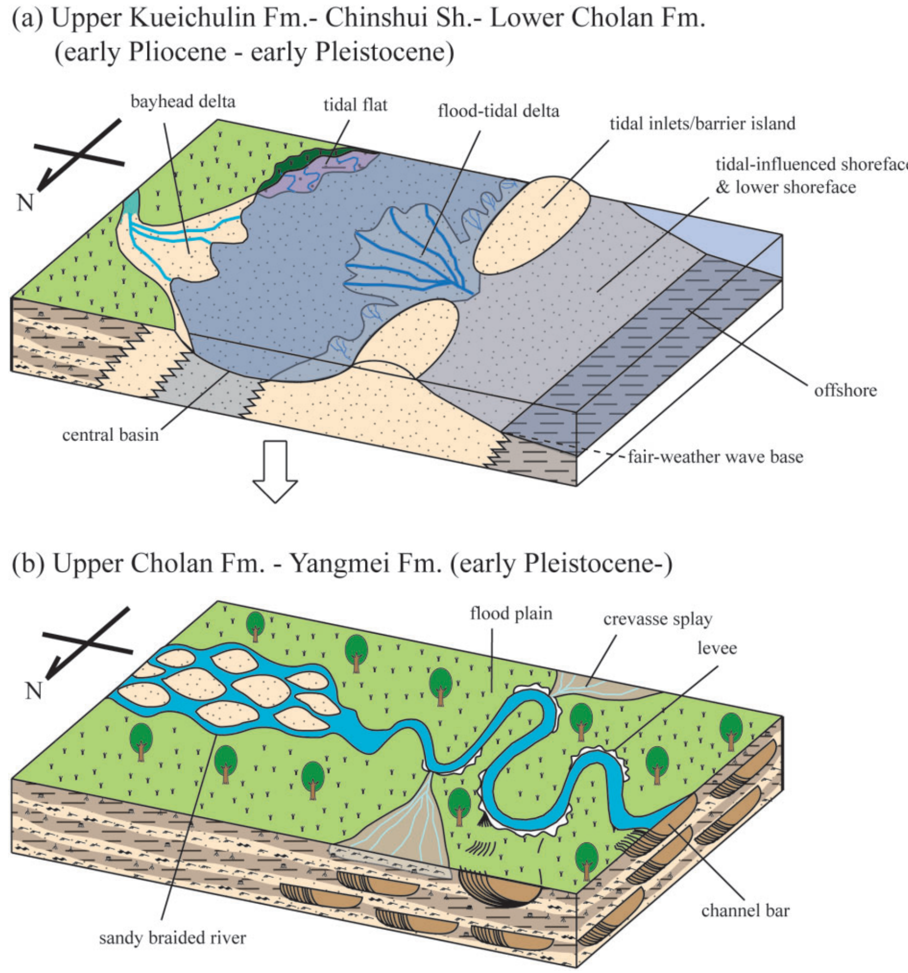

Fig. 10 Summary of depositional models developed for the studied Dahan River section. (a) During the deposition of the Kueichulin to lower Cholan Formation (early Pliocene to early Pleistocene), the foreland basin was in an open-marine to wave-dominated estuarine setting that was influenced by waves and tides. (b) During the deposition of the upper Cholan and Yangmei Formations (early Pleistocene), the basin was overfilled and the setting became a meandering and sandy braided river environment.

depositional environments of the foreland succession that occurred from approximately 4–1 Ma in the Dahan River section in NW Taiwan. The succession is characterized by 3 major depositional systems that are represented by 13 lithofacies, 17 lithofacies associations, and 2 ichnofacies. In the lower Pliocene and during the upper Kueichulin Formation stage, the succession was deposited in a wave- and tide-influenced open marine setting. In the upper Pliocene and during the Chinshui Shale stage, enhanced tectonic subsidence attributable to orogenic loading caused the foreland to become an offshore marine environment. In the Pleistocene, the lower Cholan Formation stage, the environments were shallowed to wave-dominated estuaries, indicating that the rate of basin subsidence was matched by the rate of sediment supply. In the stage of the upper Cholan Formation to Yangmei Formation, the sedimentation rate exceeded the subsidence rate, causing the foreland to become meandering and sandy braided river environments. The overall trend of the environmental evolution of this foreland succession is a deepening and then shallowing-upward trend during the Pliocene age to the Pleistocene age, spanning approximately 4–1 Ma. The studied sedimentary succession shows the interplay among the rates of basin subsidence, sediment supply, and eustatic sea-level changes. Our results indicate that the boundary between the Chinshui Shale and the Cholan Formation (roughly the NN15/NN16 boundary) signals the moment at which sediment supply began to outpace basin subsidence. Additional studies are required for understanding the origin of this rapid increase of sediment supply at the NN15/NN16 boundary.

ACKNOWLEDGEMENT

We thank Profs. Louis S. Teng and Wen-Shan Chen of National Taiwan University and Prof. Leh-Chyun Wu of Chinese Culture University for providing in-depth suggestions for this research. We appreciate the fieldwork assistance provided by Yan-Qing Li and Sheng-Ming Lin, and we

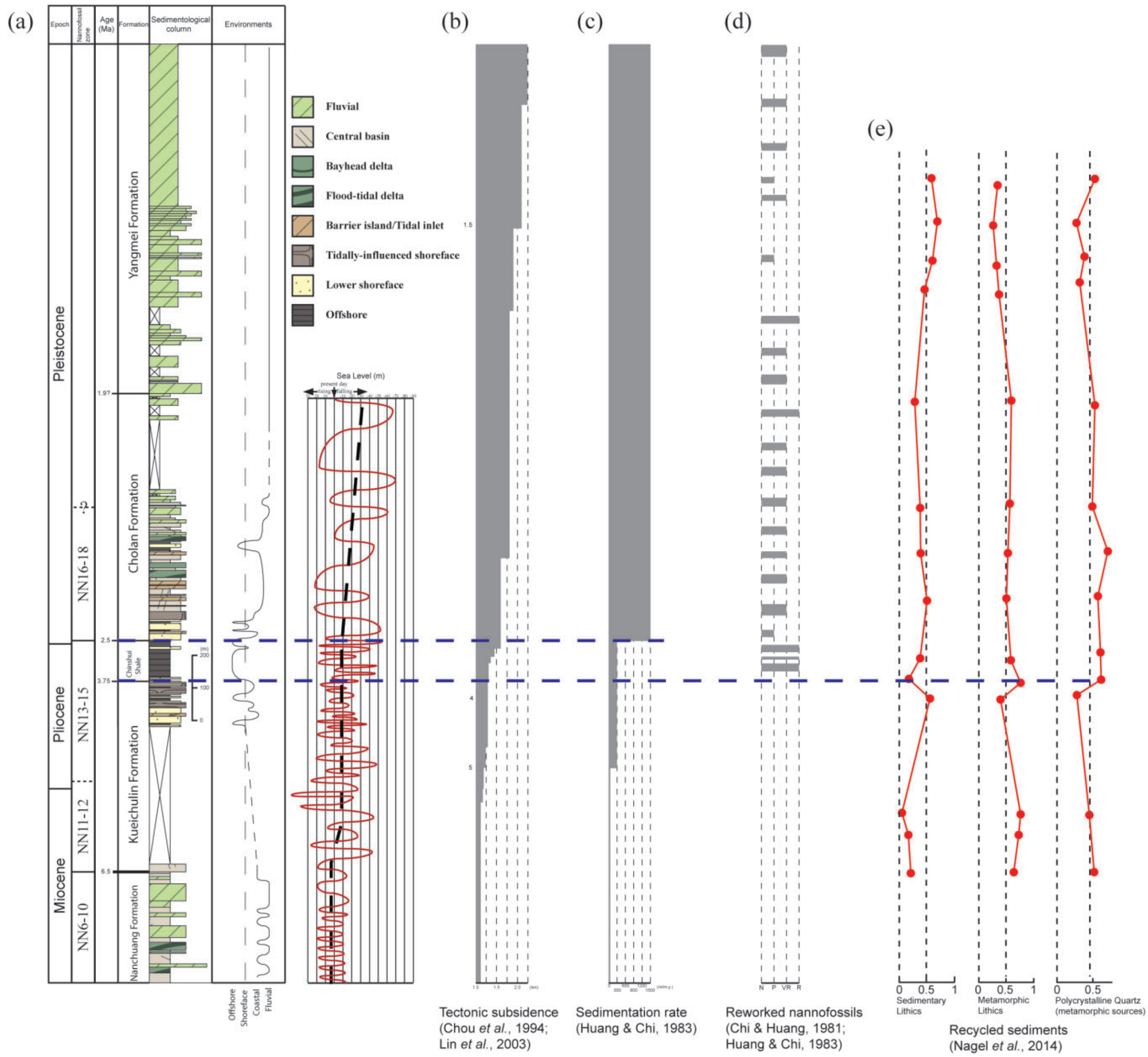

Fig. 11 Generalized stratigraphic column from the late Miocene to Pleistocene in NW Taiwan; changes of depositional environments are shown in comparison to published eustatic sea-level changes, tectonic subsidence, sedimentation rates, reworked nannofossils, and recycled sediments. (a) The environmental evolution for this succession exhibits a deepening and then a shallowing upward trend during the Pliocene to Pleistocene, whereas the eustatic sea levels remain almost stationary and exhibit several small cycles in the Pliocene and then begin declining in the Pleistocene. The eustatic sea-level changes are from Lisiecki and Raymo (2005), Miller *et al.* (2005), and Raymo *et al.* (2011). (b) The amount of tectonic subsidence increased markedly at approximately 4 Ma, implying the initiation of a phase of active orogeny (Chou *et al.* 1994; Lin *et al.* 2003). (c) The sedimentation rate increased rapidly from 250 m/ my to approximately 2000 m/my to approximately 2.5 Ma, indicating that aggradation occurred in response to the rapid subsidence and sediment supply during the Pleistocene period (Huang & Chi, 1983). (d) The appearance of reworked nannofossils suggests that the Taiwan orogenic belt has served as the main sediment source since the late Pliocene (Chang & Chi, 1983). (e) Petrographic data show an increase of lithic sedimentary fragments and a reduction of metamorphic lithic fragments, suggesting that fragments have been recycled from the Taiwan orogeny since the late Pliocene (Nagel *et al.* 2014).

thank Dr. Chii-Wen Lin of the Central Geological Survey for reviewing an early draft of the manuscript. Constructive reviews by Profs. Makato Ito, Peter Kamp, Hugh Sinclair, and an anonymous reviewer greatly improved the manuscript. This study was funded by Ministry of Science and Technology under the grant NSC 102-3113-P-008 -009.

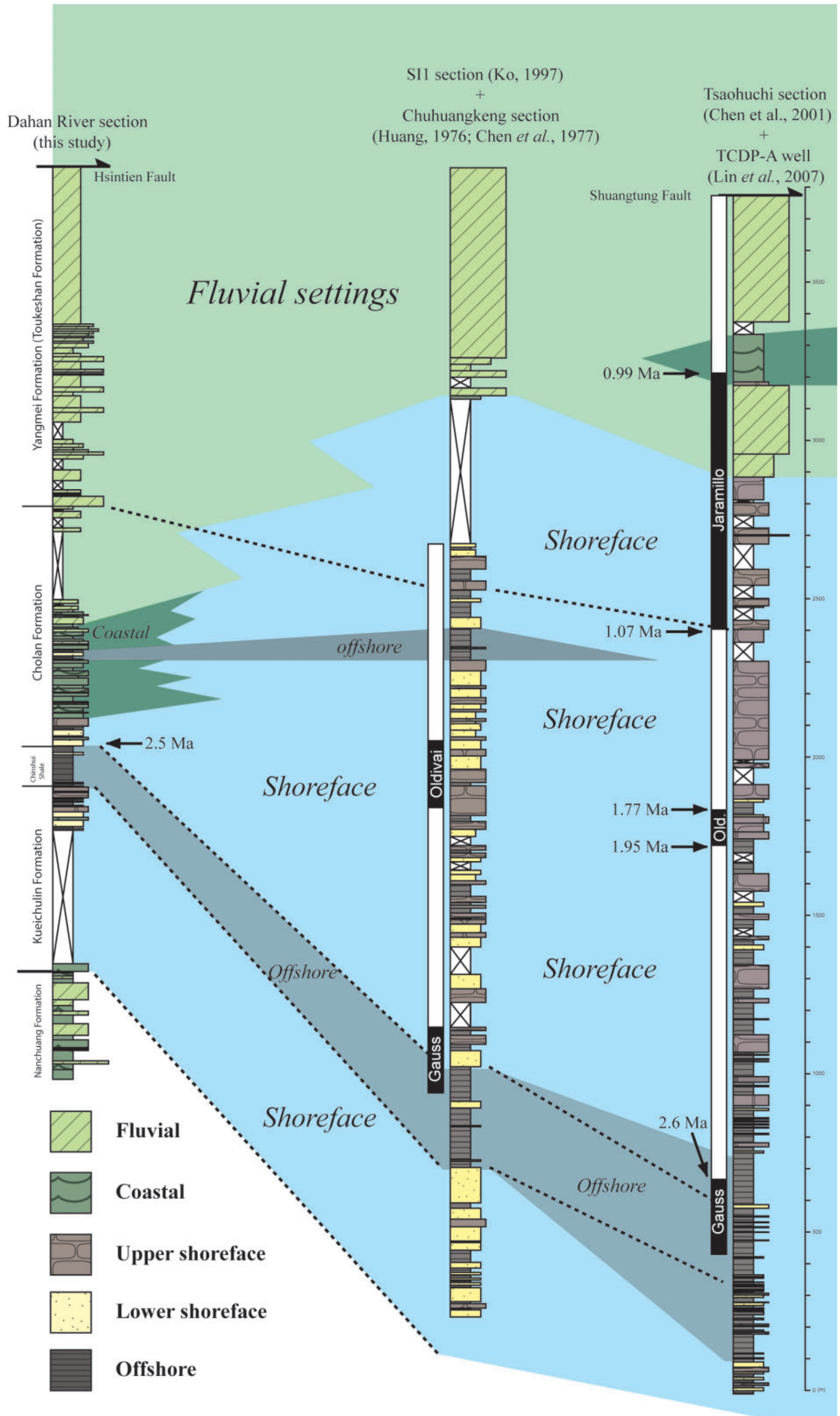

Fig. 12 Stratigraphic architecture of the foreland basin in NW and central Taiwan. In the late Pliocene, the entire Taiwan foreland basin experienced a synchronous deepening event coupled with offshore sediment accumulation (Chinshui Shale). Beginning from the early Pleistocene (i.e. since the deposition of the Cholan Formation), the basin was rapidly filled by fluvial sediments, with more pronounced and thicker offshore to shoreface deposition occurring in central Taiwan than in NW Taiwan; this is interpreted to result from the basin subsidence in central Taiwan being higher than that in NW Taiwan.

REFERENCES

Abdel-Fattah Z. A., Gingras M. K., Caldwell M. W. & Pemberton S. G. 2010. Sedimentary environments and depositional characteristics of the Middle to Upper Eocene whale-bearing succession in the Fayum Depression, Egypt. *Sedimentology* **57**, 446–76.

Backman J. 1978. Late Miocene – Early Pliocene nannofossil biochronology and biogeography in the Vera Basin SE Spain. *Stockholm Contributions in Geology* **32**, 93–114.

Beyssac O., Simoes M., Avouac J. P. *et al*. 2007. Late Cenozoic metamorphic evolution and exhumation of Taiwan. *Tectonics* **26**, TC6001. doi: 10.1029/2006TC002064.

Boggs S. Jr 2006. Marginal marine environments. *In* Boggs S. Jr (ed.) *Principles of Sedimentology and Stratigraphy*, 4th edn, pp. 289–333, Pearson Prentice Hall, Upper Saddle River, New Jersey.

Boyd R., Dalrymple R. W. & Zaitlin B. A. 2006. Estuarine and incised-valley Facies Models. *In* Posamentier H. W. and Walker R. G. (eds.) *Facies Models Revisited*, SEPM Special Publication 84, pp. 171–235, SEPM (Society of Sedimentary Geology), Tulsa, Oklahoma, U. S. A.

Catuneanu O. 2006. Stratigraphic surface. *In* Catuneanu O. (ed.) *Principles of Sequence Stratigraphy*, pp. 105–63, Elsevier, Oxford, U. K.

Chang L.-S. 1955. Stratigraphy of Taiwan. *Quarterly Journal of the Taiwan Bank* **7**, 26–49 (in Chinese).

Chang S. S.-L. & Chi W.-R. 1983. Neogene nannoplankton biostratigraphy in Taiwan and the tectonic implications. *Petroleum Geology of Taiwan* **19**, 93–147.

Chen A.-B. & Huang C.-S. 1981. *Subsurface Geology Report of Pinchen Well No. 2, Taoyuan County*. Chinese Petroleum Corporation, Taipei, Taiwan (in Chinese).

Chen P.-H., Huang T.-C., Huang C.-Y., Jiang M.-J., Lo S.-L. & Kuo C.-L. 1977. Paleomagnetic and coccolith stratigraphy of Plio-Pleistocene shallow marine sediments, Chuhuangkeng, Miaoli. *Petroleum Geology of Taiwan* **14**, 219–39.

Chen W.-S., Chung-Shin E. C.-H., Chen M.-M., Yang C.-C., Chang I.-S. & Liu T.-S. 1999. The evolution of foreland basins in the western Taiwan: Evidence from the Plio-Pleistocene Sequences. *Bulletin of the Central Geological Survey* **13**, 137–56 (in Chinese, with English abstr.).

Chen W.-S., Ridgway K. D., Horng C.-S., Chen Y.-G., Shea K.-S. & Yeh M.-G. 2001. Stratigraphic architecture, magnetostratigraphy, and incised-valley systems of Pliocene-Pleistocene collisional marine foreland basin of Taiwan. *Geological Society of America Bulletin* **113**, 1249–71.

Chi W.-R. & Huang H.-M. 1981. Nannobiostratigraphy and paleoenvironments of the late Neogene sediments and their tectonic implications in the Miaoli area, Taiwan. *Petroleum Geology of Taiwan* **18**, 111–29.

Chinese Petroleum Corporation 1978. *1:100000 Geological Map: Taoyuan – Shinchu*. Chinese Petroleum Corporation, Taiwan.

Chou S.-C., Teng L.-S., Chung H.-S. & Shiao T.-W. 1994. Geohistory analysis of west Taiwan foreland basin: A preliminary study. *Petroleum Geology of Taiwan* **29**, 289–323 (in Chinese, with English abstr.).

Clifton H. E. 2006. A reexamination of facies models for clastic shorelines. *In* Posamentier H. W. and Walker R. G. (eds.) *Facies Models Revisited*, SEPM Special Publications, 84, pp. 293–337, SEPM (Society of Sedimentary Geology), Tulsa, Oklahoma, U. S. A.

Cohen K. M. & Gibbard P. 2011. *Global Chronostratigraphical Correlation Table for the Last 2.7 Million Years*. Subcommission on Quaternary Stratigraphy (International Commission on Stratigraphy), Cambridge, England.

Collinson J. D. 1996. Alluvial sediments. *In* Reading H. G. (ed.) *Sedimentary Environments: Processes, Facies and Stratigraphy*, 3rd edn, pp. 37–82, Blackwell Publishing, Maiden, U. S. A.

Covey M. 1984. Lithofacies analysis and basin reconstruction, Plio-Pleistocene western Taiwan foredeep. *Petroleum Geology of Taiwan* **20**, 53–83.

Covey M. 1986. The evolution of foreland basins to steady state: Evidence from the western Taiwan foreland basin. *In* Allen P. A. and Homewood P. (eds.) *Foreland Basins*, Special Publication of the International Association of Sedimentologists 8, pp. 77–90, Blackwell Scientific Publications, Oxford, London, Edinburgh, Boston, Palo Alto, Melbourne.

DeCelles P. G., Gehrels G. E., Quade J. & Ojha T. P. 1998. Eocene-early Miocene foreland basin development and the history of Himalayan thrusting, western and central Nepal. *Tectonics* **17**, 741–65.

DeCelles P. G. & Giles K. A. 1996. Foreland basin systems. *Basin Research* **8**, 105–23.

Dickinson W. R. 1974. Plate tectonics and sedimentation. *In* Dickinson W. R. (ed.) *Tectonics and Sedimentation*, SEPM Special Publication 22, pp. 1–27, Society of Economic Paleontologists and Mineralogists, Tulsa, Oklahoma, U. S. A.

Ding L., Kapp P. & Wan X. 2005. Paleocene-Eocene record of ophiolite obduction and initial India-Asia collision, south central Tibet. *Tectonics* **24**, TC3001. doi:10.1029/2004TC001729.

Fielding C. R., Falker A. J. & Scott S. G. 1993. Fluvial response to foreland basin overfilling; the Late Permian Rangal Coal Measures in the Bowen Basin, Queensland, Australia. *Sedimentary Geology* **85**, 475–97.

Fuller C. W., Willett S. D., Fisher D. & Lu C. Y. 2006. A thermomechanical wedge model of Taiwan constrained by fission-track thermochronometry. *Tectonophysics* **425**, 1–24.

Gerard J. & Bromley R. G. 2008. *Ichnofabrics in Clastic Sediments: Applications to Sedimentological Core Studies: A Practical Guide*. Association des sédimentologistes français, Madrid, Spain.

Ghazi S. & Mountney N. P. 2009. Facies and architectural element analysis of a meandering fluvial succession: The Permian Warchha Sandstone, Salt Range, Pakistan. *Sedimentary Geology* **221**, 99–126.

Ghosh S. K., Chakraborty C. & Chakraborty T. 2004. Combined tide and wave influence on sedimentation of Lower Gondwana coal measures of central India: Barakar Formation (Permian), Satpura basin. *Journal of the Geological Society, London* **161**, 117–31.

Gibbard P. & Head M. J. 2009. The definition of the Quaternary System/Era and the Plesitocene Series/Epoch. *Quaternaire* **2**, 125–33.

Gingras M. K., Rasanen M. E., Pemberton S. G. & Romero L. P. 2002. Ichnology and sedimentology reveal depositional characteristics of bay-margin parasequences in the Miocene Amazonian foreland basin. *Journal of Sedimentary Research* **72**, 871–83.

Ho C.-S. 1988. *An Introduction to the Geology of Taiwan: Explanatory Text of the Geological Map of Taiwan*. Central Geological Survey, The ministry of Economic Affairs, Taiwan.

Hong E 1997. Evolution of Pliocene to Pleistocene sedimentary environments in an arc-continent collision zone: Evidence from the analyses of lithofacies and ichnofacies in the southwestern foothills of Taiwan. *Journal of Asian Earth Sciences* **15**, 381–92.

Hong E. & Wang Y. 1988. Basin analysis of the upper Miocene – lower Pliocene Series in Northern Taiwan. *Ti-Chih* **8**, 1–20 (in Chinese, with English abstr.).

Horng C.-S. & Shea K.-S. 2007. The Quaternary magentobiostratigraphy of Taiwan and Penglai Orogenic events. *Special Publication of the Central Geological Survey* **18**, 51–83 (in Chinese, with English Abstr.).

Huang S.-T., Wu J.-C., Hung J.-H. & Tanaka H. 2002. Studies of sedimentary facies, stratigraphy, and deformation structures of the Chelungpu fault zone on cores from drilled well in Fengyuan and Nantou, central Taiwan. *Terrestrial, Atmospheric and Oceanic Sciences* **13**, 253–78.

Huang T.-C. 1976. Neogene calcareous nannoplankton biostratigraphy viewed from the Chuhuankeng section, northwestern Taiwan. *Proceedings of the Geological Society of China* **19**, 7–24.

Huang T.-C. & Ting J.-S. 1981. Calcareous nannofossil biostratigraphy of the late Neogene shallow marine deposits in Taiwan. *Ti-Chih* **3**, 105–19 (in Chinese, with English abstr.).

Ko C.-T. 1997. *Depositional environments of Toukoshan Formation in San-i,Tatou and Pakwa terrace*. Master thesis, Department of Geosciences, National Taiwan University, Taiwan (in Chinese).

Kraus M.-J. 1999. Paleosols in clastic sedimentary rocks: Their geologic applications. *Earth-Science Reviews* **47**, 41–70.

Kuhlemann J. & Kempf O. 2002. Post-Eocene evolution of the North Alpine Foreland Basin and its response to Alpine tectonics. *Sedimentary Geology* **152**, 45–78.

Lin A. T., Wang S.-M., Hung J.-H., Wu M.-S. & Liu C. S. 2007. Lithostratigraphy of the Taiwan Chelungpu-fault Drilling Project-A borehole and its neighboring region, central Taiwan. *Terrestrial Atmospheric and Oceanic Sciences* **18**, 223–41.

Lin A. T. & Watts A. B. 2002. Origin of the West Taiwan Basin by orogenic loading and flexure of a rifted continental margin. *Journal of Geophysical Research* **107** (B9), 2185. doi:10.1029/2001JB000669.

Lin A. T., Watts A. B. & Hesselbo S. P. 2003. Cenozoic stratigraphy and subsidence history of the South China Sea margin in the Taiwan region. *Basin Research* **15**, 453–78.

Lisiecki L. E. & Raymo M. E. 2005. A Pliocene-Pleistocene stack of 57 globally distributed benthic $\delta^{18}O$ records. *Paleoceanography* **20**, PA1003. doi:10.1029/2004PA001071.

Liu H.-C. 1990. The division problem of Toukoushan Formation and Cholan Formation in Hsinchu-Miaoli area. *Special Publication of the Central Geological Survey* **4**, 368 (in Chinese).

Liu T.-K., Chen Y.-G., Chen W.-S. & Jiang S.-H. 2000. Rates of cooling Rates of cooling and denudation of the Early Penglai Orogeny, Taiwan, as assessed by fission-track constraints. *Tectonophysics* **320**, 69–82.

Liu T.-K., Hsieh S., Chen Y.-G. & Chen W.-S. 2001. Thermo-kinematic evolution of the Taiwan oblique-collision mountain belt as revealed by zircon fission track dating. *Earth and Planetary Science Letters* **186**, 45–56.

MacEachern J. A., Pemberton S. G., Gingras M. K. & Bann K. L. 2007. The ichnofacies paradigm: A fifty-year retrospective. *In* Miller W. III (ed.) *Trace Fossils Concepts, Problems, Prospects*, pp. 52–77, Elsevier, Oxford.

Miller K. G., Kominz M. A., Browning J. V. *et al.* 2005. The Phanerozoic record of global sea-level change. *Science* **310**, 1293–8.

Nagel S., Castelltort S., Garzanti E. *et al.* 2014. Provenance evolution during Arc–continent collision: Sedimentary petrography of miocene to pleistocene sediments in the western foreland basin of Taiwan. *Journal of Sedimentary Research* **84**, 513–28.

Nagel S., Castelltort S., Wetzel A., Willett S. D., Mouthereau F. & Lin A. T. 2013. Sedimentology and foreland basin paleogeography during Taiwan arc-continent collision. *Journal of Asian Earth Science* **60**, 180–204.

Najman Y., Bickle M., Garzanti E. *et al.* 2009. Reconstructing the exhumation history of the Lesser

Himalaya, NW India, from a multitechnique provenance study of the foreland basin Siwalik Group. *Tectonics* **28**, TC5018. doi:10.1029/2009TC002506.

Najman Y., Johnson K., White N. & Olivers G. 2004. Evolution of the Himalayan foreland basin, NW India. *Basin Research* **16**, 1–24.

Naylor M. & Sinclair H. D. 2008. Pro- vs. retro-foreland basins. *Basin Research* **20**, 285–303.

Nichols G. 2009. Rivers and alluvial fans. *In* Nichols G. (ed.) *Sedimentology and Stratigraphy*, 2nd edn, pp. 129–50, Wiley-Blackwell, West Sussex, U. K.

Pan T.-Y. 2011. *A Study on Sedimentary Environments of Nanchuang Formation to Yangmei Formation along the Dahan River Section, Northwestern Taiwan*. Master thesis, Graduate Institute of Geophysics, National Central University, Taiwan (in Chinese, with English abstr.).

Pemberton S. G., Splia M., Pulham A. J. *et al*. 2001. *Ichnology & Sedimentology of Shallow to Marginal Marine Systems: Ben Nevis & Avalon Reservoirs, Jeanne D'arc Basin*. Geological Association of Canada Short Course Notes.

Raymo M. E., Mitrovica J. X., O'Leary M. J., DeConto R. M. & Hearty P. J. 2011. Departures from eustasy in Pliocene sea-level records. *Nature Geoscience* **4**, 328–32.

Reading H. G. & Collinson J. D. 1996. Clastic coasts. *In* Reading H. G. (ed.) *Sedimentary Environments: Processes, Facies and Stratigraphy*, 3rd edn, pp. 154–231, Blackwell Publishing, Maiden, U. S. A.

Reinson G. E. 1992. Transgressive barrier island and estuarine systems. *In* Walker R. G. and James N. (eds.) *Facies Models: Response to Sea Level Change*, 3rd edn, pp. 179–94, Geological Association of Canada, St. John's, Canada.

Roddaz M., Brusset S., Baby P. & Herail G. 2006. Miocene tidal-influenced sedimentation to continental Pliocene sedimentation in the forebulge-backbulge depozones of the Beni-Mamore foreland Basin (northern Bolivia). *Journal of South American Earth Sciences* **20**, 351–68.

Shao P.-H. 2009. Correlation and division of Pleistocene stratigraphy in north-central Taiwan. *Special Publication of the Central Geological Survey* **22**, 115–47 (in Chinese, with English abstr.).

Shea K.-S. & Huang T. 2003. Tertiary stratigraphy in Taiwan. *The Taiwan Mining Industry* **55**, 17–32 (in Chinese).

Simoes M. & Avouac J. P. 2006. Investigating the kinematics of mountain building in Taiwan from the spatiotemporal evolution of the foreland basin and western foothills. *Journal of Geophysical Research* **111**, B10401. doi:10.1029/2006JB004824.

Simoes M., Avouac J. P., Beyssac O., Goffé B., Farley K. A. & Chen Y.-G. 2007. Mountain building in Taiwan: A thermokinematic model. *Journal of Geophysical Research* **112**, B11405. doi:10.1029/2006JB004824.

Sinclair H. D. 1997. Tectonostratigraphic model for underfilled peripheral foreland basins: An Alpine perspective. *Geological Society of America Bulletin* **109**, 324–46.

Tang C.-H. 1962. *Preliminary Report of Subsurface Geology of KY-1 Well, Taoyuan County*. Chinese Petroleum Corporation, Taipei, Taiwan (in Chinese).

Tang C.-H. 1963. Contemporaneous deformation in the Pleistocene Yangmei Formation of the Hukou Area, Hsinchu. *Proceedings of the Geological Society of China* **6**, 75–9.

Tang C.-H. 1964. Subsurface geology and oil possibilities of the Taoyuan district. *Petroleum Geology of Taiwan* **3**, 53–73.

Teng L.-S. 1987. Stratigraphic records of the late Cenozoic Penglai Orogeny of Taiwan. *Acta Geologica Taiwanica Science Reports of the National Taiwan University* **25**, 205–24.

Teng L.-S. 1990. Geotectonic evolution of late Cenozoic arc-continent collision in Taiwan. *Tectonophysics* **183**, 57–76.

Ting H.-H., Huang C.-Y. & Wu L.-C. 1991. Paleoenvironments of the late Neogene sequences along the Nantzuhsien River, southern Taiwan. *Petroleum Geology of Taiwan* **26**, 121–49.

Tu M.-K. & Chen W.-C. 1984. Facies associations of the Yangmei Formation in the Chaomen area, Hukou. *Bulletin of the Central Geological Survey* **3**, 57–71.

Tu M.-K., Lin C.-C. & Chen W.-C. 1984. The depositional environment of the Cholan Formation in the Takeng area near Taichung. *Special Publication of the Central Geological Survey* **3**, 61–73 (in Chinese, with English abstr.).

Tu M.-K. & Shao P.-H. 2001. *Geologic Map of Taiwan Sheet No. 7, Chungli*, 2nd edn, Central Geological Survey, MOEA, Zhonghe, Taiwan (in Chinese, with English abstr.).

Walker R. G. & Plint A. G. 1992. Wave- and storm-dominated shallow marine systems. *In* Walker R. G. and James N. P. (eds.), *Facies Models: Response to Sea Level Change*, 3rd edn pp. 219–38, Geological Association of Canada, St. John's, Canada.

Wu L.-C. 1993. *Sedimentary Basin Succession of the Upper Neogene and Quaternary Series in the Chishan Area, Southern Taiwan, and Its Tectonic Evolution*. Ph.D. Thesis of National Taiwan University, Taipei (in Chinese).

Wu L.-C. & Wang Y. 1989. Depositional environments of the upper Miocene to lower Pleistocene series in the Yunshuichi section, Chia Yi area, Taiwan. *Ti-Chih* **9**, 15–43 (in Chinese, with English abstr.).

Yang S.-H. & Hong E. 1994. The Sedimentary environments of the Plio-Pleistocene Series in the Liushuang-Chailiao area, southwestern Foothills of Taiwan based on lithofacies analysis. *Special Publication of Central Geological Survey* **8**, 41–63 (in Chinese, with English abstr.).

Yu H.-S. & Chou Y.-W. 2001. Characteristics and development of the flexural forebulge and basal unconformity of western Taiwan foreland basin. *Tectonophysics* **333**, 277–91.

Yu N.-T. & Teng L.-S. 1996. Facies characteristics and depositional cycles of Middle and Upper Miocene strata of the Western Foothills, Northern Taiwan. *Ti-Chih* **15**, 29–60 (in Chinese, with English abstr.).